In order to measure amounts of the polymer chains that were not included in the PFC-emulsions, we carried out the following experiment. PFC-emulsion was prepared in the conditions of Run 4 of Table 2; polymer: F-59%, sample volume: 300 μL, polymer concentration: 4 wt.%, PFC5: 2 vol.%, PFC6: 2 vol.%, sonication at 40 °C for 3 min. The obtained emulsion was transferred into a 1.5 mL Eppendorf-type poly(propylene) tube and centrifuged at 13,200 rpm for 5 min with an Eppendorf centrifuge model 5415D (Eppendorf Co., Ltd. Japan, Tokyo, Japan). The emulsion was found to precipitate at the bottom. 200 μL of the supernatant was collected and freeze-dried. We calculated the polymer amounts that were not included in the PFC-emulsions by multiplying 1.5 (=300 μL/200 μL) to the freeze-dried polymer weight. As a control, we carried out the same experiment just only for the polymer (without addition of TFC5 nor TFC6).

2.4. Measurements

2.4.1. Dynamic light scattering (DLS)
The size of emulsions was measured with a dynamic light scattering (DLS) instrument, the DLS-7000 (Otsuka Electronics, Tokyo, Japan). DLS samples were prepared through appropriate dilution of the emulsions with commercial distilled water for internal injection (Otsuka Pharmaceutical Co. Ltd., Tokyo, Japan). The measurements were made at 25 °C, and scattering was observed at a 90° angle with respect to the incident beam. The cumulant average particle size and the particle size distribution from a non-negative least square method were determined by the use of software provided with the instrument.

2.4.2. Gas chromatography
We measured concentrations of PFC5 using two gas chromatograph systems as described below. In both cases, we successfully obtained clear separation of PFC5's peak from PFC6's peak, and carried out quantitative analyses using a standard sample of PFC5. Therefore, the two gas chromatograph systems gave us identical results. However, we only used the (2) system described below for blood samples because its pre-heating function was essential for measurements of blood samples.

2.4.2.1. Gas chromatograph system.
We measured PFC5 using a gas chromatograph model G-6000 (Hitachi High-Technologies Corporation, Tokyo, Japan) equipped with a Gaskuropack 54 80/100 packed column (GL Sciences, Inc., Tokyo, Japan) and an FID detector at 200 °C. Carrier gas was nitrogen at a flow rate of 300 mL/min. 5 μL of a sample solution were injected into the gas chromatograph system with a micro syringe at 0 min. Column temperature was controlled in the following manner; 100 °C (0 min), raised at a rate of 5 °C/min until 130 °C (6 min), and then raised at a rate of 60 °C/min until 190 °C (7 min), followed by maintenance of 190 °C for 2 min. PFC5 and PFC6 were found to elute at 3.8 min and 6.4 min, respectively.

2.4.2.2. Gas chromatograph system.
We measured PFC5 using a gas chromatograph system GC-2014 (Shimadzu Corp., Kyoto, Japan) equipped with an FID detector at 250 °C. We used two tandem-connected two columns: DB-WAX 127-7012 (Agilent Technologies Japan, Ltd., Tokyo, Japan) and RESTEK Rt-QBond 19741 (Shimadzu GLC Ltd., Tokyo, Japan). Carrier gas was helium at a flow rate of 20 mL/min. Either 100 or 544 μL of a sample solution were heated at 200 °C and injected with a headspace autosampler TurboMatrix Trap 40 (PerkinElmer Japan Co., Ltd., Yokohama, Japan). Column temperature was constant at 150 °C. PFC5 and PFC6 were found to elute at 3.6 min and 4.4 min, respectively.

2.5. Measurements of PFC5 concentration in blood

In vivo PFC5 concentration profiles in blood were evaluated in Balb/c female mice (6 weeks old). 100 μL of PFC-emulsion was intravenously administered via lateral tail veins. The emulsions' PFC5 concentrations ranged from 0.429 to 0.670 vol.%. Blood (44 μL) was collected with a heparinized blood-collecting glass tube, and mixed with 500 μL of heparin solution in a capped sample tube of the (2) gas chromatograph system.

3. Results

3.1. General characteristics of the emulsion-preparation method with a bath-type sonicator

In representative conditions, we successfully obtained PFC5-containing nano-sized emulsions having diameters of ca. 200 nm in considerably high PFC5 yields. Fig. 3(a) and (b) shows diameter distributions measured by means of dynamic light scattering (DLS) for PEG-P(Asp(C7F9)59) (F-59% in Table 1). In these conditions, we dissolved 12.0 mg of polymer in 300 μL water (4.0 wt.% solution), and put this polymer solution in a 1.5 mL glass vial, followed by additions of 6 μL (corresponding to 2.0 vol.% of water) of PFC5 and 6 μL of PFC6. Sonication was performed for 3 min in a bath-type sonicator at 40 °C. In the first three preparations (run 6 in Table 2), the cumulant diameter obtained was 205.5 ± 15.8 nm (the average ± standard deviation; $n = 3$), and Fig. 3(a) shows the weight-weighted diameter distribution of one preparation. Almost uniformly distributed emulsions were obtained, and the diameter of the emulsion droplets had a very small size about 200 nm. In this run 6, PFC5 concentrations were 0.682 ± 0.074 vol.%. These values are considered large enough for ultrasound images (Kawabata et al., 2005, 2010a,b). In another set of three preparations (on another day, run 7 in Table 2), we obtained a very similar average diameter, 173.5 ± 24.5 nm (the average ± standard deviation; $n = 3$) and PFC5 concentrations. The diameter distribution of one preparation of run 7 is shown in Fig. 3(b). These two figures exhibited a major peak at about 200 nm, while a minor peak was seen in a larger diameter side and a smaller diameter side, as shown in Fig. 3(a) and (b), respectively. This difference may result from a slight variation in sonication conditions such as the position of samples and the water level of the sonicator. These emulsions were obtained and measured without any purification process after the sonication, and a large majority of the emulsions in weight were found to have a diameter of about 200 nm. All these results clearly indicate that this sonication method brought about very small nanometer-sized PFC5-containing emulsions with considerably high PFC5 concentrations.

We measured a proportion of polymer incorporated in the PFC-emulsion out of the feed polymer amount. In these preparation conditions (run 7 in Table 2), 75.4 ± 2.6% ($n = 3$) of the feed polymer was found in a supernatant obtained after centrifugation. (All the PFC-emulsions were observed to precipitate in this centrifugation.) When this measurement was carried out for the polymer alone, 93.8 ± 2.0% ($n = 3$) of the feed polymer was found in a supernatant obtained after centrifugation. Therefore, 18.4% (=93.8%–75.4%) of the feed polymer was considered to be incorporated into the PFC-emulsions. Removal of the free polymer chain, that was not incorporated into the PFC-emulsion, was not examined in this study. The removal is difficult because the free polymer existed as a polymeric micelle was close to the PFC-emulsion in size. (If the free polymer existed as a single polymer chain, a difference in size between the free polymer and the PFC-emulsion would be so large to allow separation such as ultrafiltration.)
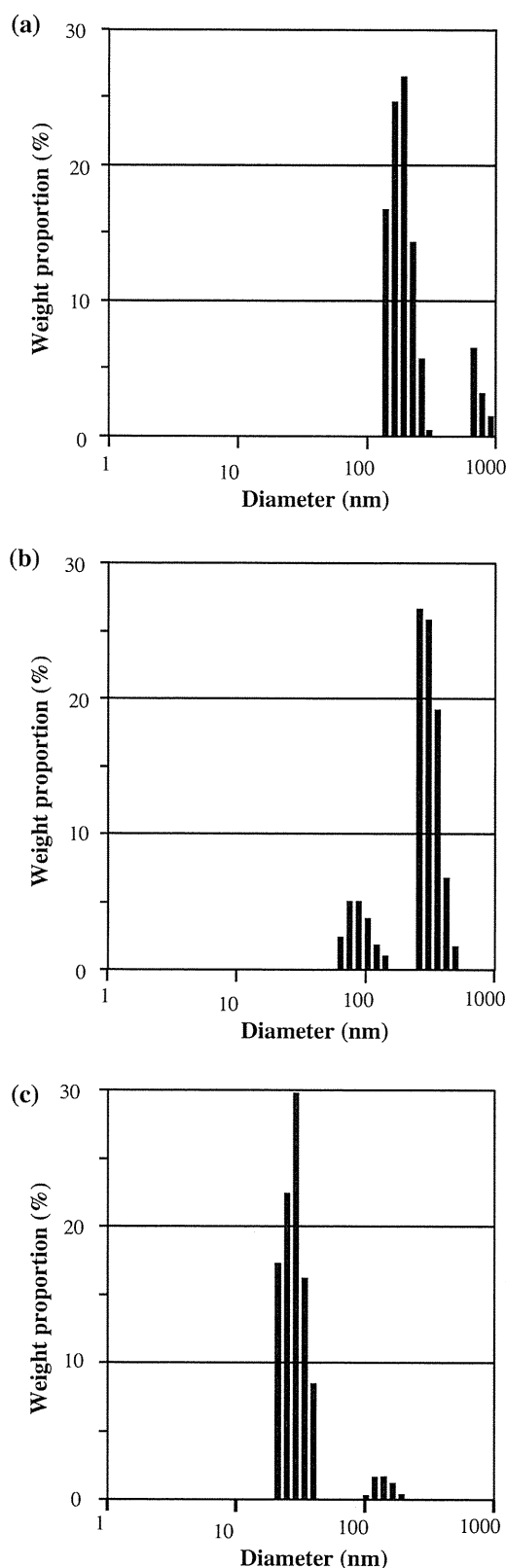
Fig. 3. Diameter distribution of PFC5-containing nano-emulsions (a and b) forming from PEG-P(Asp(C7F9)59) and empty polymeric micelle (c) measured by means of DLS. (a and b) are of different batches but prepared in the same conditions.

Using this polymer amount incorporated into the PFC-emulsions, we calculated the thickness of the polymer shell. We carried out the calculation with the following assumptions.

(1) The PFC-emulsions are made of the two phases; the inner PFC droplet phase and the outer polymer shell phase.
(2) We obtained PFC6 amounts in the emulsions assuming that sensitivity of PFC6 in gas chromatography is the same as that of PFC5. (The same peak area per PFC volume.)
(3) PFC6 and PFC5 are mixed freely without any gain or loss of droplet volume.
(4) Density of polymer is 1.03. (This is a common value of protein, and most synthetic polymers show similar values.)

The obtained value of the polymer shell's thickness was 22 nm, while the radius of the PFC droplet was 65 nm. In the future study, we like to analyse relationships between the shell thickness and physical stability of the emulsions.

3.2. Comparison with other emulsion-preparation methods

We compared the PFC5's concentrations of the PFC5-containing emulsions prepared in the sonication method with the PFC5's concentrations of the emulsions prepared in two common methods; mechanical stirring and high-pressure emulsification (Solans et al., 2005). We also compared the diameters of the emulsions prepared in the sonication method with those prepared in the two common methods. Previously, we reported PFC5-containing emulsions prepared by means of mechanical stirring that featured a magnetic stirrer (Nishihara et al., 2009). In this method, only the F-14% polymer provided a high PFC5 concentration (0.65 vol.%). The other polymers provided low or very low PFC5 concentrations: F-6% had 0.28 vol.%, F-22% had 0.19 vol.%, F-39% had 0.02 vol.%, and F-67% had 0.01 vol.%. In the F-14% case, the cumulant diameter was 694 nm, which was much larger than those obtained in the sonication method as described in the previous section (Section 3.1). Another distinct difference was found in a wide range of polymer compositions for high PFC5 concentrations in the sonication method. As summarized in runs 1–5 of Table 2, we compared the PFC5 concentrations (vol.%) and average diameters of the PFC5-containing emulsions for five polymer compositions. All these five compositions of polymers provided high PFC5 concentrations larger than 0.6 vol.%. Furthermore, all emulsion sizes of these runs (runs 2–5) were revealed to be small, at about 200 nm.

In the next step, we compared the sonication method with the most common method for emulsion preparation:high-pressure emulsification. For this comparison, we used F-15% polymer. We compared PFC5 concentrations and the cumulant average diameters of the emulsions prepared in the sonication method with PFC5 concentrations and the cumulant average diameters of the "high-pressure method" emulsions. We acquired a considerably high PFC5 concentration, 0.58 vol.%, by using a high-pressure emulsifier for the high-pressure emulsification method (its procedure is described in Section 2.3.1). However, the cumulant average diameter of the obtained emulsion was 477 nm. This value was much larger than the sonication-method value (232.4 nm, run 2 of Table 2). Additionally, maintenance of a low temperature at 4 °C for the whole instrument was essential in the high-pressure emulsification method, since possible heat generation due to the high-pressure process may considerably boost evaporation of PFC5 (the boiling temperature of PFC5 is 29 °C). In contrast, in the sonication method, a high PFC5 concentration was obtained at 40 °C, which is above PFC5's boiling temperature. (The temperature issue of the emulsion-preparation process will be more closely examined in the following section (Section 3.4).)
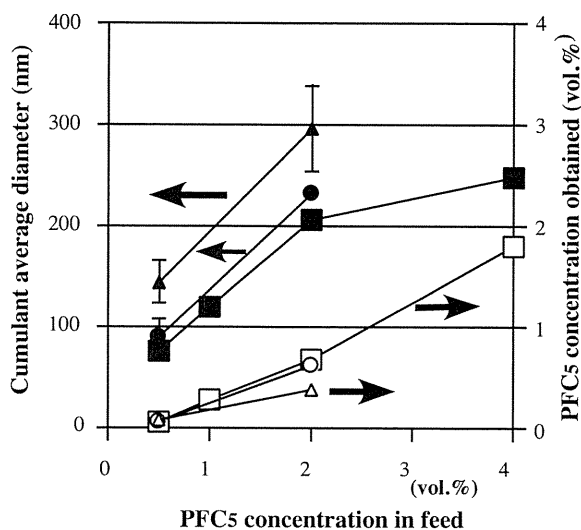
Fig. 4. Effects of polymer and PFC5 concentrations on physical properties of emulsions. PEG-P(Asp(C7F9)59) was used for emulsion preparations. Sample volume was 300 μL in 1.5-mL sample vials. Sonication was performed for 3 min at 40 °C. Filled plots represent cumulant average diameters, and vacant plots represent PFC5 concentrations of emulsions. Polymer concentration: △, ▲: 1.0 vol.%; ○, ●: 2.0 vol.%; □, ■: 4.0 vol.%.

All these results indicate that the sonication method is a facile method for preparations of PFC5-containing emulsions with very small nano-sizes and high PFC5 concentrations.

3.3. Effects of sample volume, polymer concentration, and PFC5 concentration on incorporation behaviors

In the standard conditions, we put 300 μL water in a 1.5-mL of sealed glass tube and added polymer, PFC5, and PFC6. This configuration meant that a considerable amount of PFC5 perhaps would move from the solution into the glass tube's vacant atmospheric space (ca. 1.2 mL). We changed the volume of water while keeping constant the concentrations of polymer, PFC5, and PFC6 in the tube. Table 2 summarizes the results of runs 6–9 of Table 2. A higher PFC5 concentration was obtained in a case involving a larger water volume. (This means that there was a smaller vacant space in a sealed tube.) In accordance with the higher concentration of PFC5, the average diameter of the emulsion was observed to be larger. In run 9, PFC5's yield reached a very high value, approximately 90%. On the other hand, the PFC5's yield decreased to 32–33% when a small sample volume (300 μL) was adopted. These values indicate that the emulsification process can be well controlled through adjustment of sample volume.

Then, we examined effects that both polymer concentrations and PFC5 concentrations in feed had on the two physical values: diameter and PFC5 concentrations of the emulsion. Fig. 4 shows results of these two physical values for F-59% polymer cases. We changed the polymer concentration and the PFC5 concentration in feed in a range of 1.0–4.0 wt.% and of 0.5–4.0 vol.%, respectively. Each empty plot indicates PFC5 concentrations obtained for each polymer concentration, while each filled plot indicates cumulant average diameters for each polymer concentration. The polymer concentration was not found to significantly affect these two physical values. The polymer concentration affected very slightly the PFC5 content because three plot lines almost overlapped. When the polymer concentration was raised, only a small drop in the cumulant average diameter was observed. In contrast, the PFC5 concentration in feed was revealed to greatly affect the two physical values; larger values of PFC5 concentrations and cumulant average diameters were obtained with larger PFC5 concentrations in
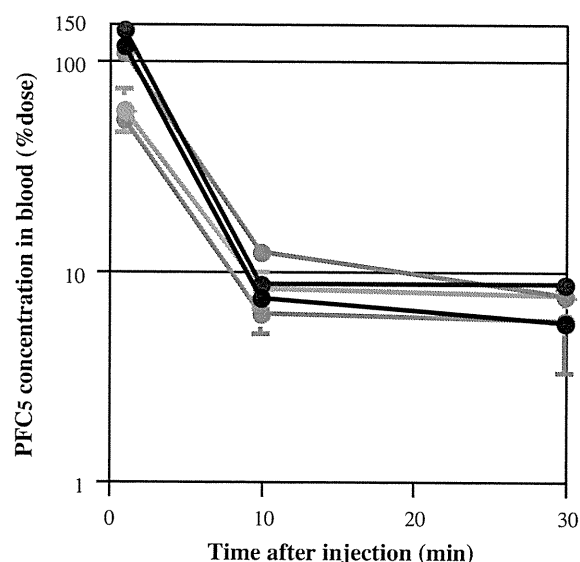

Fig. 5. Profiles of PFC5 concentration in blood. Black plot: run 1; blue plot: run 2; green plot: run 3; yellow plot: run 4; and red plot: run 5 (Table 5).

feed. Diameters of multi-modal distributions like Fig. 3(a) and (b) cannot be evaluated with the cumulant average diameters because the cumulant average diameters suppose the uni-modal diameter distribution. Therefore, we evaluated weight-weighted diameter distributions. Supplementary data, Table A summarizes and compares weight-weighted diameters with the cumulant average diameters. In most emulsion preparations, diameter distributions were found to be bi- or tri-modal, and therefore, exactly quantitative measurements of weight-weighted diameters are difficult in the homodyne analysis of dynamic light scattering done in this study. In fact, considerable differences are observed between the weight-weighted diameters and the cumulant average diameters for emulsions prepared in low PFC5 feed concentrations such as 1%, possibly due to the presence of empty polymeric micelles. (A DLS result of the empty micelle is shown in Fig. 3(c).) Even in this technical difficulty, the correlations obtained in Fig. 4a are not changed when multi-modal distributions are compared in the Supplementary data, Table A.

From the results obtained in this section, it was revealed that the sample volume and the PFC5 concentration in feed were appropriate factors for the facile control of size and the PFC5 content of the nano-sized emulsion.

3.4. Function of PFC6 in an emulsion preparation

In the above-described procedures for the emulsion preparation, we always used a 1:1 (vol./vol.) mixture of PFC5 and PFC6 in order to obtain a high PFC5 yield at a temperature higher than the boiling temperature of PFC5. We chose this 1:1 ratio because Kawabata et al. reported that ultrasound intensity required for the phase-transition (vaporization) induction at the 1:1 ratio was similar to that of a PFC5 alone case, and that this intensity was almost constant between ratios of 15:85, 50:50 (=1:1), and 85:15 (Asami et al., 2009). We varied temperatures (15, 25, 40, and 65 °C) of a sonicator's water bath, and performed the emulsion preparation both in the presence and the absence of PFC6 at each temperature. Table 3 summarizes results. In the absence of PFC6, PFC5 concentration was smaller than that of the corresponding PFC6-present case at every temperature. In runs 2 and 4, the obtained emulsions contained a considerable quantity of PFC5 over 0.2 vol.%. These two runs were prepared at lower temperatures than a boiling temperature of PFC5 (29 °C). Only a very small amount of PFC5

Table 3
Effects of temperature and PFC6 addition on PFC5 incorporation behaviors.

Run	Temperature (°C)	PFC6 addition	PFC5 concentration (vol.%)[a]	Cumulant average diameter (nm)[a]
1	15	Yes	0.727 ± 0.191	210.8 ± 17.8
2	15	No	0.419 ± 0.124	82.7 ± 2.6
3	25	Yes	0.566 ± 0.367	177.1 ± 8.9
4	25	No	0.205 ± 0.086	95.7 ± 8.9
5[b]	40	Yes	0.634 ± 0.361	173.5 ± 24.5
6	40	No	0.049 ± 0.059	98.5 ± 5.1
7	65	Yes	0.154 ± 0.051	136.2 ± 16.0
8	65	No	0.096[c]	303.7[c]

[a] Average ± standard deviation ($n = 3$) except run 8.
[b] This run is identical to run 6 of Table 2.
[c] Average of two preparations.

was incorporated in run 6, which was performed at 40 °C, which is above PFC5's boiling temperature. This indicates that most PFC5 evaporated at 40 °C, and that interfacial Laplace pressure did not suppress PFC5's evaporation in the sonication procedure possibly because PFC5 evaporated from macroscopic PFC's droplets (in mm scale) before its incorporation into nano-emulsions where Laplace pressure's effect is great. In contrast, the PFC6-present cases presented similar amounts of PFC5 incorporated at 15, 25, and 40 °C. This means that PFC5's evaporation at 40 °C was efficiently suppressed through the mixing with PFC6. PFC5 and PFC6 not only are miscible but also these two compounds are expected to strongly interact with each other because these are both perfluorocarbons. It is considered that PFC5 evades evaporation through the strong interaction with PFC6 that has a higher boiling temperature than 40 °C. In run 7, performed at 65 °C, a considerable drop in the incorporated PFC5 amount was seen. This sonication temperature (65 °C) is higher than PFC6's boiling temperature (60 °C), and therefore, both PFC5 and PFC6 were evaporated at 65 °C. From these results, we have confirmed the function of the added PFC6 for high PFC5-incorporation amounts at a temperature higher than PFC5's boiling temperature.

3.5. PFC5 concentration profile in blood

We measured PFC concentrations in blood using several PFC5-containing emulsions in order to control their pharmacokinetic behaviors. For a larger amount of emulsion accumulation at tumor tissues, a longer half-life is preferable for a contrast agent. In contrast, a shorter half-life is advantageous for a diagnosis in a short period after injection of a contrast injection, since a low concentration of the contrast agent in blood is a pre-requisite for a high contrast image of the contrast agent's accumulated region. Under this contradictory situation for the optimum half-life, it is very important to obtain technologies to control (prolong and shorten) a half-life of the contrast agent.

We used three different types of polymers including PEG-P(Asp(C7F9)x) block copolymers in order to control half-livers in blood. In Table 4, we describe the compositions of the two

Table 4
Compositions of two poly(L-lactic acid)(PLA)-containing polymers.

Code	Structure	Compositions
Gelatin derivative	Poly(L-lactic acid)-grafted gelatin	M.W. of PLA: 1000 weight ratio PLA/gelatin = 0.17
PEG-PLA	Poly(ethylene glycol)-b-Poly(L-lactic acid) Block copolymer	M.W. of PEG: 2000 M.W. of PLA: 1000

copolymers other than PEG-P(Asp(C7F9)x). These two copolymers contain hydrophobic poly(L-lactic acid) chains that are expected to work for incorporation of hydrophobic PFC5 into emulsions. Table 5 summarizes five samples prepared from four polymers. By adjusting the vacant volume of a 1.5-mL glass vial to a small value (ca., 300 μL, meaning 1.2 mL of the sample volume.), we successfully obtained emulsions with higher PFC5 contents than 0.4 vol.% in runs 1–3. In these cases, the sonication was carried out at 15 °C. When emulsions were prepared in the same conditions of run 1 except for a different temperature (at 40 °C) and a different vacant volume (ca. 0 μL), the PFC5 content was considerably lower (0.408 vol.%) than in run 1.

We injected these five samples in a mouse tail vein. As shown in Fig. 5, we observed a distinct difference in PFC5 concentrations at 1 min after the injection between three runs containing PLA (runs 1–3) and the other two runs for PEG-P(Asp(C7F9)x). The former three runs showed almost a 100% dose at 1 min with an assumption that blood volume was 7 vol./wt.% of body weight, while the latter two runs provided considerably smaller values than the 100% dose. In all runs, however, PFC5 concentrations were rapidly lowered at 10 and 30 min after the injection, and no clear difference was observed at these time points among all the runs. Therefore, control of pharmacokinetic behaviors, in particular prolongation of blood half-life from a few minutes, was not successfully achieved in this examination by the use of different polymer structures. For the pharmacokinetic control of the emulsions, an additional functional component may be required. Rapoport et al. (Rapoport et al., 2011) reported a very stable circulation (half-life = 2–4 h) in blood for perfluoro-crown-ether compound containing nano-emulsions.

Table 5
Compositions of PFC-emulsions for in vivo experiments.

Run	Polymer	Polymer concentration in feed (%)[a]	PFC5 concentration in feed (vol.%)	PFC5 concentration obtained in emulsion (vol.%)	Cumulant average diameter (nm)
1	Gelatin derivative[b]	1.0	1.25[d]	0.613	345.9
2	Gelatin derivative[b]	4.0	1.25[d]	0.429	542.6
3	PEG-b-PLA[a]	4.0	1.0[d]	0.491	222.6
4	F-15%[c]	4.0	2.0	0.465	256.3
5	F-59%[c]	4.0	1.0	0.670	225.1

[a] Weight (g)/water volume (mL).
[b] Listed in Table 4.
[c] Listed in Table 1.
[d] Sonication at 15 °C.

According to this report, a perfluoro compound showing stable emulsion formation may be utilized for stable incorporation of another PFC.

4. Discussion

In the examinations of this study, we successfully obtained very small (ca. 200 nm in diameter) PFC5-containing emulsions with high PFC5 contents in a very facile method using a common bath-type sonicator. Actually, the used sonicator was the smallest model with the lowest sonication power (max. Input power: 90 W) in its product line. The other facile aspect of this preparation method is the working temperature. By mixing PFC6 we performed the emulsion preparation at 40 °C, which is above the boiling temperature of PFC5. In a conventional method's use of a high-pressure emulsifier, cooling of the whole system is required for evading a large amount evaporation of PFC5 due to heat generated within a high-pressure emulsifier. In contrast, we did not need cooling samples during the preparation. This facileness is substantially important when we consider a scale-up of the emulsion preparations. In a large-scale production of these emulsions, the heat generated in preparation processes (both in emulsification and sonication) may become large enough to raise a temperature of the solution above the boiling temperature. Therefore, successful preparations at a high temperature means that there is a large margin for large-scale preparation with high PFC5 content as well as easy handling of samples at room temperature throughout the sonication procedure.

We could not substantially change pharmacokinetic behaviors of the PFC5-containing emulsion, even when using different polymers. This is a very different situation from polymeric micelle drug carrier cases where block polymer structure was revealed to be a very influential factor on pharmacokinetic behaviors of the incorporated drug into the polymeric micelles (Yokoyama, 2005, 2007; Watanabe et al., 2006). This difference may result from the liquid state of the emulsion's core, while the solid core is essential for stable drug incorporation in the polymeric micelle systems. An alternative and novel method may be required to obtain stable incorporation of liquid PFC for dramatically changed pharmacokinetics.

5. Conclusion

By using a bath-type sonicator, we successfully obtained PFC5-containing emulsions in a diameter range of 200 nm. These emulsions are very potent for theranostics of solid tumors through ultrasound irradiation. Furthermore, these emulsions were prepared in high PFC5 yields at 40 °C, which is higher than the boiling temperature of PFC5. This very facile preparation method is an important technological key for large-scale production of these medically valuable emulsions.

Acknowledgements

Appendix A. Supplementary data

Supplementary data associated with this article can be found, in the online version, at doi:10.1016/j.ijpharm.2011.10.006.

References

Ai, H., 2011. Layer-by-layer capsules for magnetic resonance imaging and drug delivery. Adv. Drug Deliv. Rev. 63, 772–788.

Asami, R., Azuma, T., Kawabata, K., 2009. Fluorocarbon droplets as next generation contrast agents—their behavior under 1–3 mhz ultrasound. IEEE Proc. Int. Ultrasonics Symp., 1294–1297.

Asami, R., Ikeda, T., Azuma, T., Kawabata, K., Umemura, S., 2010. Acoustic signal characterization of phase change nanodroplets in tissue-mimicking phantom gels. Jpn. J. Appl. Phys. 49, 07HF16.

Blanco, E., Kessinger, C.W., Sumer, B.D., Gao, J., 2009. Multifunctional micellar nanomedicine for cancer therapy. Exp. Biol. Med. 234, 123–131.

Bryson, J.M., Fichter, K.M., Chu, W.J., Lee, J.H., Li, J., Madsen, L.A., McLendon, P.M., Reineke, T.M., 2009. Polymer beacons for luminescence and magnetic resonance imaging of DNA delivery. Proc. Natl. Acad. Sci. U.S.A. 106, 16913–16918.

Chen, X.S., 2011. Introducing theranostics journal—from the editor-in-chief. Theranostics 1, 1–2.

Gianella, A., Jarzyna, P.A., Mani, V., Ramachandran, S., Calcagno, C., Tang, J., Kann, B., Dijk, W.J., Thijssen, V.L., Griffioen, A.W., Storm, G., Fayad, Z.A., Mulder, W.J., 2011. A multifunctional nanoemulsion platform for imaging guided therapy evaluated in experimental cancer. ACS Nano 5, 4422–4433.

Grishenkov, D., Pecorari, C., Brismar, T.B., Paradossi, G., 2009. Characterization of acoustic properties of PVA-shelled ultrasound contrast agents: ultrasound-induced fracture (part II). Ultrasound Med. Biol. 35, 1139–1147.

Hernot, S., Klibanov, A.L., 2008. Microbubbles in ultrasound-triggered drug and gene delivery. Adv. Drug Deliv. Rev. 60, 1153–1166.

Ishida, O., Maruyama, K., Sasaki, K., Iwatsuru, M., 1999. Size-dependent extravasation and interstitial localization of polyethyleneglycol liposomes in solid tumor-bearing mice. Int. J. Pharm. 190, 49–56.

Jeong, H., Huh, M., Lee, S.J., Koo, H., Kwon, I.C., Jeong, S.Y., Kim, K., 2011. Photosensitizer-conjugated human serum albumin nanoparticles for effective photodynamic therapy. Theranostics 1, 230–239.

Kaida, S., Cabral, H., Kumagai, M., Kishimura, A., Terada, Y., Sekino, M., Aoki, I., Nishiyama, N., Tani, T., Kataoka, K., 2010. Visible drug delivery by supramolecular nanocarriers directing to single-platformed diagnosis and therapy of pancreatic tumor model. Cancer Res. 70, 7031–7041.

Kalber, T.L., Kamaly, N., Higham, S.A., Pugh, J.A., Bunch, J., McLeod, C.W., Miller, A.D., Bell, J.D., 2011. Synthesis and characterization of a theranostic vascular disrupting agent for in vivo MR imaging. Bioconjug. Chem. 22, 879–886.

Kamaly, N., Miller, A.D., 2010. Paramagnetic liposome nanoparticles for cellular and tumour imaging. Int. J. Mol. Sci. 11, 1759–1776.

Kawabata, K., Sugita, N., Yoshikawa, H., Azuma, T., Umemura, S., 2005. Nanoparticles with multiple perfluorocarbons for controllable ultrasonically induced phase shifting. Jpn. J. Appl. Phys. 44, 4548–4552.

Kawabata, K., Asami, R., Yoshikawa, H., Azuma, T., Umemura, S., 2010a. Acoustic response of microbubbles derived from phase-change nanodroplet. Jpn. J. Appl. Phys. 49, 07HF18.

Kawabata, K., Asami, R., Yoshikawa, H., Azuma, T., Umemura, S., 2010b. Sustaining microbubbles derived from phase change nanodroplet by low-amplitude ultrasound exposure. Jpn. J. Appl. Phys. 49, 07HF20.

Kim, K., Kim, J.H., Park, H., Kim, Y.S., Park, K., Nam, H., Lee, S., Park, J.H., Park, R.W., Kim, I.S., Choi, K., Kim, S.Y., Park, K., Kwon, I.C., 2010. Tumor-homing multifunctional nanoparticles for cancer theragnosis: simultaneous diagnosis, drug delivery, and therapeutic monitoring. J. Contr. Rel. 146, 219–227.

Lammers, T., Kiessling, F., Hennink, W.E., Storm, G., 2010. Nanotheranostics and image-guided drug delivery: current concepts and future directions. Mol. Pharm. 7, 1899–1912.

Lammers, T., Aime, S., Hennink, W.E., Storm, G., Kiessling, F., 2011. Theranostic Nanomedicines. Acc. Chem. Res. 44, 1029–1038.

Litzinger, D.C., Buiting, A.M.J., van Rooijen, N., Huang, L., 1994. Effect of liposome size on the circulation time and intraorgan distribution of amphipathic poly(ethylene glycol)-containing liposomes. Biochim. Biophys. Acta 1190, 99–107.

MacKay, J.A., Li, Z., 2010. Theranostic agents that co-deliver therapeutic and imaging agents? Adv. Drug Deliv. Rev. 62, 1003–1004.

Min, K.H., Kim, J.H., Bae, S.M., Shin, H., Kim, M.S., Park, S., Lee, H., Park, R.W., Kim, I.S., Kim, K., Kwon, I.C., Jeong, S.Y., Lee, D.S., 2010. Tumoral acidic pH-responsive MPEG-poly(beta-amino ester) polymeric micelles for cancer targeting therapy. J. Contr. Rel. 144, 259–266.

Mohan, P., Rapoport, N., 2010. Doxorubicin as a molecular nanotheranostic agent: effect of doxorubicin encapsulation in micelles or nanoemulsions on the ultrasound-mediated intracellular delivery and nuclear trafficking. Mol. Pharm. 6, 1959–1973.

Moon, G.D., Choi, S.W., Cai, X., Li, W., Cho, E.C., Jeong, U., Wang, L.V., Xia, Y., 2011. A new theranostic system based on gold nanocages and phase-change materials with unique features for photoacoustic imaging and controlled release. J. Am. Chem. Soc. 133, 4762–4765.

Nagayasu, A., Uchiyama, K., Nishida, T., Yamagiwa, Y., Kawai, Y., Kiwada, H., 1996. Is control of distribution of liposomes between tumors and bone marrow possible? Biochim. Biophys. Acta 1278, 29–34.

Nakamura, E., Makino, K., Okano, T., Yamamoto, T., Yokoyama, M., 2006. A polymeric micelle MRI contrast agent with changeable relaxivity. J. Contr. Rel. 114, 325–333.

Nishihara, M., Imai, K., Yokoyama, M., 2009. Preparation of perfluorocarbon/fluoroalkyl polymer nanodroplets for cancer-targeted ultrasound contrast agents. Chem. Lett. 38, 556–557.

Opanasopit, P., Yokoyama, M., Watanabe, M., Kawano, K., Maitani, Y., Okano, T., 2004. Block copolymer design for camptothecin incorporation into polymeric micelles for passive tumor targeting. Pharm. Res. 21, 2003–2010.

Pan, D., Caruthers, S.D., Hu, G., Senpan, A., Scott, M.J., Gaffney, P.J., Wickline, S.A., Lanza, G.M., 2008. Ligand-directed nanobialys as theranostic agent for drug delivery and manganese-based magnetic resonance imaging of vascular targets. J. Am. Chem. Soc. 130, 9186–9187.

Rapoport, N., Gao, Z., Kennedy, A., 2007. Multifunctional nanoparticles for combining ultrasonic tumor imaging and targeted chemotherapy. J. Natl. Cancer Inst. 99, 1095–1106.

Rapoport, N.Y., Kennedy, A.M., Shea, J.E., Scaife, C.L., Nam, K.H., 2009a. Controlled and targeted tumor chemotherapy by ultrasound-activated nanoemulsions/microbubbles. J. Contr. Rel. 138, 268–276.

Rapoport, N.Y., Nam, K.H., Gao, Z., Kennedy, A., 2009b. Application of ultrasound for targeted nanotherapy of malignant tumors. Acoust. Phys. 55, 594–601.

Rapoport, N., Christensen, D.A., Kennedy, A.M., Nam, K.H., 2010a. Cavitation properties of block copolymer stabilized phase-shift nanoemulsions used as drug carriers. Ultrasound Med. Biol. 36, 419–429.

Rapoport, N., Kennedy, A.M., Shea, J.E., Scaife, C.L., Nam, K.H., 2010b. Ultrasonic nanotherapy of pancreatic cancer: lessons from ultrasound imaging. Mol. Pharm. 7, 22–31.

Rapoport, N., Nam, K.H., Gupta, R., Gao, Z., Mohan, P., Payne, A., Todd, N., Liu, X., Kim, T., Shea, J., Scaife, C., Parker, D.L., Jeong, E.K., Kennedy, A.M., 2011. Ultrasound-mediated tumor imaging and nanotherapy using drug loaded, block copolymer stabilized perfluorocarbon nanoemulsions. J. Contr. Rel. 153, 4–15.

Sanson, C., Diou, O., Thévenot, J., Ibarboure, E., Soum, A., Brûlet, A., Miraux, S., Thiaudière, E., Tan, S., Brisson, A., Dupuis, V., Sandre, O., Lecommandoux, S., 2011. Doxorubicin loaded magnetic polymersomes: theranostic nanocarriers for MR imaging and magneto-chemotherapy. ACS Nano 5, 1122–1140.

Schutt, E.G., Klein, D.H., Mattrey, R.M., Riess, J.G., 2003. Injectable microbubbles as contrast agents for diagnostic ultrasound imaging: the key role of perfluorochemicals. Angew. Chem. Int. Ed. Engl. 42, 3218–3235.

Shiraishi, K., Kawano, K., Minowa, T., Maitani, Y., Yokoyama, M., 2009. Preparation and in vivo imaging of PEG-poly(L-lysine)-based polymeric micelle MRI contrast agents. J. Contr. Rel. 136, 14–20.

Shiraishi, K., Kawano, K., Maitani, Y., Yokoyama, M., 2010. Synthesis of Poly(ethylene glycol)-b-poly(L-lysine) block copolymers having Gd-DOTA as MRI contrast agent and their polymeric micelle formation by polyion complexation. J. Contr. Rel. 148, 160–167.

Solans, C., Izquierdo, P., Nolla, J., Azemar, N., Garcia-Celma, M.J., 2005. Nano-emulsions. Curr. Opin. Colloid Interface Sci. 10, 102–110.

Tadros, T., Izuquierdo, P., Esquena, J., Solans, C., 2004. Formation and stability of nano-emulsions. Adv. Colloid Interface. Sci. 108–109, 303–318.

Tanigo, T., Takaoka, R., Tabata, Y., 2010. Sustained release of water-insoluble simvastatin from biodegradable hydrogel augments bone regeneration. J. Contr. Rel. 143, 201–206.

Unger, E.C., Porter, T., Culp, W., Labell, R., Matsunaga, T., Zutshi, R., 2004. Therapeutic applications of lipid-coated microbubbles. Adv. Drug Deliv. Rev. 56, 1291–1314.

Yamamoto, T., Yokoyama, M., Opanasopit, P., Hayama, A., Kawano, K., Maitani, Y., 2007. What are determining factors for stable drug incorporation into polymeric micelle carriers? Consideration on physical and chemical characters of the micelle inner core. J. Contr. Rel. 123, 11–18.

Yokoyama, M., 2005. Polymeric micelles for the targeting of hydrophobic drugs. In: Kwon, G.S. (Ed.), Drug and Pharmaceutical Sciences, Polymeric Drug Delivery Systems, 148. Taylor & Francis, Boca Raton, pp. 533–575.

Yokoyama, M., 2007. Polymeric micelles as nano-sized drug carrier systems. In: Domb, A.J., Tabata, Y., Kumar, M.N.V.R., Farber, S. (Eds.), Nanoparticles for Pharmaceutical Applications. American Scientific Publishers, Stevenson Ranch, pp. 63–72.

Yokoyama, M., Opanasopit, P., Maitani, Y., Kawano, K., Okano, T., 2004. Polymer design and incorporation method for polymeric micelle carrier system containing water-insoluble anti-cancer agent camptothecin. J. Drug Target. 12, 373–384.

Yuan, F., Dellian, M., Fukumura, D., Leunig, M., Berk, D.A., Torchilin, V.P., Jain, R.K., 1995. Vascular permeability in a human tumor xenograft: molecular size dependence and cutoff size. Cancer Res. 55, 3752–3756.

Watanabe, M., Kawano, K., Yokoyama, M., Opanasopit, P., Okano, T., Maitani, Y., 2006. Preparation of camptothecin-loaded polymeric micelles and evaluation of their incorporation and circulation stability. Int. J. Pharm. 308, 183–189.

Suppression of Melanoma Growth and Metastasis by DNA Vaccination Using an Ultrasound-Responsive and Mannose-Modified Gene Carrier

Keita Un,[†,‡] Shigeru Kawakami,[*,†] Ryo Suzuki,[§] Kazuo Maruyama,[§] Fumiyoshi Yamashita,[†] and Mitsuru Hashida[*,†,∥]

[†]Department of Drug Delivery Research, Graduate School of Pharmaceutical Sciences, Kyoto University, 46-29 Yoshida-shimoadachi-cho, Sakyo-ku, Kyoto 606-8501, Japan

[‡]The Japan Society for the Promotion of Science (JSPS), Chiyoda-ku, Tokyo 102-8471, Japan

[§]Department of Biopharmaceutics, School of Pharmaceutical Sciences, Teikyo University, 1091-1 Suwarashi, Midori-ku, Sagamihara, Kanagawa 252-5195, Japan

[∥]Institute for Integrated Cell-Material Sciences (iCeMS), Kyoto University, Yoshida-ushinomiya-cho, Sakyo-ku, Kyoto 606-8302, Japan

Ⓢ Supporting Information

ABSTRACT: DNA vaccination has attracted much attention as a promising therapy for the prevention of metastasis and relapse of malignant tumors, especially highly metastatic tumors such as melanoma. However, it is difficult to achieve a potent cancer vaccine effect by DNA vaccination, since the number of dendritic cells, which are the major targeted cells of DNA vaccination, is very few. Here, we developed a DNA vaccination for metastatic and relapsed melanoma by ultrasound (US)-responsive and antigen presenting cell (APC)-selective gene carriers reported previously, named Man-PEG$_{2000}$ bubble lipoplexes. Following immunization using US exposure and Man-PEG$_{2000}$ bubble lipoplexes constructed with pUb-M, which expresses ubiquitylated melanoma-specific antigens (gp100 and TRP-2), the secretion of Th1 cytokines (IFN-γ

and TNF-α) and the activities of cytotoxic T lymphocytes (CTLs) were specifically enhanced in the presence of B16BL6 melanoma antigens. Moreover, we succeeded in obtaining potent and sustained DNA vaccine effects against solid and metastatic tumor derived from B16BL6 melanoma specifically. The findings obtained from this study suggest that the gene transfection method using Man-PEG$_{2000}$ bubble lipoplexes and US exposure could be suitable for DNA vaccination aimed at the prevention of metastatic and relapsed cancer.

KEYWORDS: mannose modification, bubble lipoplex, ultrasound, DNA vaccination, melanoma
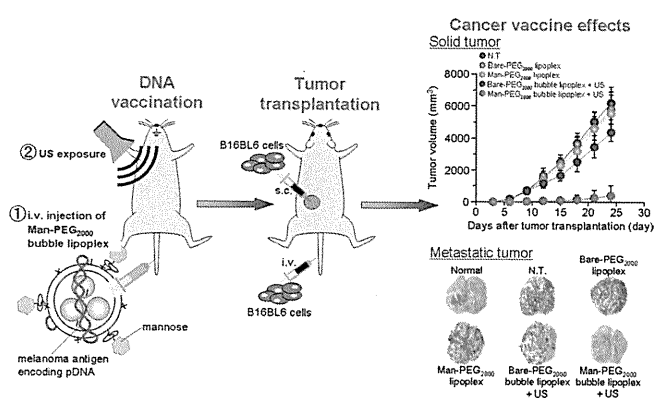
■ INTRODUCTION

Melanoma is a neoplasm arising within epidermal melanocytes of the skin, and one of several cancers exhibiting the increasing incidence in recent years.[1] Early stage melanoma is curable, but melanoma metastasis and relapse occur frequently in the patients following treatments such as surgery, and the prognosis for patients with metastatic melanoma is poor.[2,3] Although systemic therapy induces complete therapeutic responses in a minority of patients, metastatic melanoma is a devastating illness and treatment options are limited; therefore, there is a need for an effective therapy for metastatic melanoma.

Cancer vaccination has attracted much attention as a promising therapy for the prevention of tumor growth and metastasis, because it is based on an immune response provided by the cancer antigen, and consequently, its therapeutic effects are specific to the targeted cancer cells and the adverse effects followed by

cancer vaccination are low.[4,5] In particular, it has been reported that DNA vaccination, which uses an exogenous gene encoding cancer antigen, can induce not only humoral immunity but also cellular immunity and, moreover, can induce cancer-specific CTLs with potent antitumor activities.[6–9] In a variety of cancers, since melanoma is known to exhibit inherent immunogenicity and the identification of melanoma-specific antigen is proceeding, such as gp100, melanoma-antigen recognized by T cells-1 (MART-1) and tyrosinase-related protein (TRP),[10–13] it is considered that DNA vaccination against melanoma is suitable for not only the

prevention of metastasis and relapse but also the suppression of tumor growth.

To achieve potent therapeutic effects by DNA vaccination against cancer, it is essential to transfer the antigen-coding gene selectively and efficiently into APCs such as macrophages and dendritic cells, which play a pivotal role in the initiation, programming and regulation of cancer-specific immune responses.[14,15] Our group has also developed mannose-modified liposome/plasmid DNA (pDNA) complexes (mannose-modified lipoplexes) for APC-selective gene transfer via mannose receptors expressing on APCs, and obtained APC-selective gene expression in the liver and spleen by mannose-modified lipoplexes.[16,17] Moreover, our group also succeeded in obtaining DNA vaccine effects against cancer by intraperitoneal administration of mannose-modified lipoplexes constructed with tumor-specific antigen coding pDNA, such as ovalbumin (OVA) and melanoma-related antigens.[18,19] However, the gene transfection efficiency into APCs was lower than that in other cells;[20] therefore, it could be difficult to induce a potent cancer vaccine effect for the prevention of metastasis and relapse by DNA vaccination using conventional lipofection methods.

It has been reported that cancer vaccine effects can be enhanced by physical stimulation-mediated gene transfer such as electroporation,[21,22] hydrodynamic injection[23,24] and sonoporation methods.[25] These transfection methods enable the delivery of a large amount of antigen-coding gene and antigen peptides into APCs, since exogenous materials are directly introduced into the cytoplasm without endocytosis in these methods.[26-29] Recently, we have applied "sonoporation methods[25,29-31]" using US exposure and microbubbles enclosing US imaging gas to enhance gene expression in APCs[32] and developed a gene transfection method for DNA vaccination using US-responsive and mannose-modified gene carriers, Man-PEG$_{2000}$ bubble lipoplexes.[33] This method enables APC-selective and -efficient gene expression, and moreover, effective vaccine effects against OVA-expressing cancer cells were obtained by applying this method to DNA vaccination using OVA-encoding pDNA.[33] However, the antigenicity of OVA is extremely high compared with other antigens,[34] and it is difficult to extrapolate the result obtained by DNA vaccination against OVA-expressing cells to actual cancer therapy, since OVA-expressing cells are transfectant constructed by gene transfer. Therefore, it is unclear if DNA vaccination by gene transfer using Man-PEG$_{2000}$ bubble lipoplexes and US exposure is effective against cancer, i.e. melanoma, with metastatic properties.

In this study, we examined DNA vaccine effects against melanoma by transfection of pUb-M, coexpressing ubiquitylated gp100 and TRP-2, using Man-PEG$_{2000}$ bubble lipoplexes and US exposure. First, we examined the level of gene expression in the splenic dendritic cells by gene transfer using Man-PEG$_{2000}$ bubble lipoplexes constructed with pUb-M and US exposure. Second, we studied the characteristics of cytokine secretion and the induction of CTL activities against B16BL6 cell-derived melanoma by DNA vaccination using Man-PEG$_{2000}$ bubble lipoplexes constructed with pUb-M and US exposure. Then, we investigated the cancer vaccine effects against solid and metastatic tumors derived from B16BL6 cells by DNA vaccination using Man-PEG$_{2000}$ bubble lipoplexes and US exposure. Finally, we evaluated the duration of cancer vaccine effects against solid and metastatic melanoma after pUb-M transfection using Man-PEG$_{2000}$ bubble lipoplexes and US exposure.

EXPERIMENTAL SECTION

Materials. 1,2-Stearoyl-3-trimethylammoniumpropane (DSTAP), 1,2-distearoyl-sn-glycero- 3-phosphocholine (DSPC) and 1,2-distearoyl-sn-glycero-3-phosphoethanolamine-N-[amino-(polyethylene glycol)-2000] (NH$_2$-PEG$_{2000}$-DSPE) were purchased from Avanti Polar Lipids Inc. (Alabaster, AL, USA), Sigma Chemicals Inc. (St. Louis, MO, USA) and NOF Co. (Tokyo, Japan), respectively. Anti-CD11c monoclonal antibody (N418)-labeled magnetic beads were obtained from Miltenyi Biotec Inc. (Auburn, CA, USA). Fetal bovine serum (FBS) was purchased from Equitech-bio Inc. (Kerrville, TX, USA). RPMI-1640 and Dulbecco's modified Eagle's medium (DMEM) were purchased from Nissui Pharmaceutical Co., Ltd. (Tokyo, Japan). All other chemicals were of the highest purity available.

pDNA, Cell Lines and Mice. pUb-M containing murine melanoma glycoprotein-100$_{25-33}$ (gp100) and tyrosinase-related protein-2$_{181-188}$ (TRP-2) peptide epitopes was kindly provided by Prof. R. A. Reisfeld.[35] The B16BL6 melanoma cells, colon-26 adenocarcinoma cells and EL4 lymphoma cells were obtained from American Type Culture Collection (ATCC, Manassas, VA, USA). The B16BL6/Luc cells and colon-26/Luc cells, which are cell lines expressing firefly luciferase stably, were established as previously reported.[36,37] The B16BL6 cells and EL4 cells were cultured in DMEM, and the colon-26 cells were cultured in RPMI-1640 at 37 °C in 5% CO$_2$. Both media were supplemented with 10% FBS, 100 IU/mL penicillin, 100 μg/mL streptomycin, and 2 mM L-glutamine. Female C57BL/6 mice (6 weeks old) and female Balb/c mice (6 weeks old) were purchased from the Shizuoka Agricultural Cooperative Association for Laboratory Animals (Shizuoka, Japan). All animal experiments were carried out in accordance with the Principles of Laboratory Animal Care as adopted and propagated by the U.S. National Institutes of Health and the Guidelines for Animal Experiments of Kyoto University.

Construction of Man-PEG$_{2000}$ Bubble Lipoplexes. Man-PEG$_{2000}$ bubble lipoplexes were constructed according to our previous report.[33] Briefly, DSTAP, DSPC and NH$_2$-PEG$_{2000}$-DSPE or mannose-modified PEG$_{2000}$-DSPE were mixed in chloroform at a molar ratio of 7:2:1 to produce the liposomes for bubble lipoplexes. The mixture for construction of liposomes was dried by evaporation and vacuum desiccated, and the resultant lipid film was resuspended in sterile 5% dextrose. After hydration for 30 min at 65 °C, the dispersion was sonicated for 10 min in a bath sonicator and for 3 min in a tip sonicator to produce liposomes. Then, the liposomes were sterilized by passage through a 0.45 μm filter (Nihon-Millipore, Tokyo, Japan). The lipoplexes were prepared by gently mixing equal volumes of pDNA and liposome solution at a charge ratio of 1.0:2.3 ($-$:$+$). To enclose US imaging gas in lipoplexes, the prepared lipoplexes were pressured with perfluoropropane gas (Takachiho Chemical Industries Co., Ltd., Tokyo, Japan) and sonicated using a bath-type sonicator (AS ONE Co., Osaka, Japan) for 5 min. The particle sizes and zeta potentials of the liposomes/lipoplexes were determined by a Zetasizer Nano ZS instrument (Malvern Instrument, Ltd., Worcestershire, U.K.).

In Vivo Gene Transfection Method. Six week old C57BL/6 female mice were intravenously injected with 400 μL of bubble lipoplexes via the tail vein using a 26 gauge syringe needle at a dose of 50 μg of pDNA. At 5 min after the injection of the bubble lipoplexes, US (frequency, 1.045 MHz; duty, 50%; burst rate,

Table 1. Particle Sizes and Zeta Potentials of Lipoplexes and Bubble Lipoplexes Constructed with pUb-M[a]

	particle size (nm)	zeta-potential (mV)
Bare-PEG$_{2000}$ lipoplex (DSTAP:DSPC:NH$_2$-PEG$_{2000}$-DSPE = 7:2:1 (mol))	144 ± 13	45.7 ± 4.5
Man-PEG$_{2000}$ lipoplex (DSTAP:DSPC:Man-PEG$_{2000}$-DSPE = 7:2:1 (mol))	143 ± 10	44.5 ± 5.8
Bare-PEG$_{2000}$ bubble lipoplex (DSTAP:DSPC:NH$_2$-PEG$_{2000}$-DSPE = 7:2:1 (mol))	557 ± 20	46.7 ± 4.2
Man-PEG$_{2000}$ bubble lipoplex (DSTAP:DSPC:Man-PEG$_{2000}$-DSPE = 7:2:1 (mol))	555 ± 19	45.1 ± 2.2

[a] Each value represents the mean ± SD ($n = 3$).

10 Hz; intensity 1.0 W/cm^2; time, 2 min) was exposed transdermally to the abdominal area using a Sonopore-4000 sonicator with a probe of diameter 20 mm. At predetermined times after injection, mice were sacrificed and spleens were collected for each experiment. In the intradermal transfection study, mice were intradermally injected with 200 μL of bubble lipoplexes at a dose of 50 μg of pDNA. At 5 min after the injection of the bubble lipoplexes, US (frequency, 2.062 MHz; duty, 50%; burst rate, 10 Hz; intensity 4.0 W/cm^2; time, 2 min) was directly exposed to the injected site using a probe of diameter 6 mm. In the intrasplenic transfection, mice were directly injected into the spleen with 200 μL of bubble lipoplexes at a dose of 50 μg of pDNA. At 5 min after the injection of the bubble lipoplexes, US (frequency, 2.062 MHz; duty, 50%; burst rate, 10 Hz; intensity 4.0 W/cm^2; time, 2 min) was directly exposed to the spleen using a probe of diameter 6 mm.

Measurement of the Level of mRNA Expression. Total RNA was isolated from the spleen using a GenElute Mammalian Total RNA Miniprep Kit (Sigma-Aldrich, St. Louis, MO, USA). Reverse transcription of mRNA was carried out using a Prime-Script RT reagent Kit (Takara Bio Inc., Shiga, Japan). The detection of the Ub-M cDNA was carried out by real-time PCR using SYBR Premix Ex Taq (Takara Bio Inc., Shiga, Japan) and Lightcycler Quick System 350S (Roche Diagnostics, Indianapolis, IN, USA) with primers. The primers for Ub-M, gp100, TRP-2 and GAPDH cDNA were constructed as follows: primer for Ub-M cDNA, 5'-GAG CCC AGT GAC ACC ATA GA-3' (forward) and 5'-GTG CAG GGT GGA CTC TTT CT-3' (reverse); primer for gp100, 5'-GCA CCC AAC TTG TTG TTC CT-3' (forward) and 5'-GTG CTA CCA TGT GGC ATT TG-3' (reverse); primer for TRP-2, 5'-CTT CCT AAC CGC AGA GCA AC-3' (forward) and 5'-CAG GTA GGA GCA TGC TAG GC-3' (reverse); primer for GAPDH, 5'-TCT CCT GCG ACT TCA ACA-3' (forward) and 5'-GCT GTA GCC GTA TTC ATT GT-3' (reverse) (Sigma-Aldrich, St. Louis, MO, USA). The mRNA copy numbers were calculated for each sample from the standard curve using the instrument software ("Arithmetic Fit Point analysis" for the Lightcycler). Results were expressed as relative copy numbers calculated relative to GAPDH mRNA (copy numbers of Ub-M, gp100 and TRP-2 mRNA/copy numbers of GAPDH mRNA).

Isolation of Splenic CD11c$^+$ Cells (Dendritic Cells) in Mice. At 6 h after transfection, spleens were harvested and spleen cells were suspended in ice-cold RPMI-1640 medium on ice. Then, red blood cells were removed by incubation with hemolytic reagent (0.15 M NH$_4$Cl, 10 mM KHCO$_3$, 0.1 mM EDTA) for 3 min at room temperature. CD11c$^+$ and CD11c$^-$ cells were separated by magnetic cell sorting with an auto MACS (Miltenyi Biotec Inc., Auburn, CA, USA) following the manufacturer's instructions.

Evaluation of Antigen-Specific Cytokine Secretion. To prepare the tumor cell lysates (B16BL6 cells, EL4 cells and colon-26 cells), the cells were scraped from the plates and suspended in lysis buffer (0.05% Triton X-100, 2 mM EDTA, 0.1 M Tris, pH 7.8). After three cycles of freezing and thawing, the lysates were centrifuged at 10000g, 4 °C for 10 min and the resultant supernatants were collected. The protein concentration of cell lysates was determined with a Protein Quantification Kit (Dojindo Molecular Technologies, Inc., Tokyo, Japan). At 2 weeks after the last immunization, the splenic cells collected from immunized mice were plated in 96-well plates and incubated for 72 h at 37 °C in the presence or absence of tumor cell lysates (100 μg of proteins). IFN-γ, TNF-α, IL-4 and IL-6 in the culture medium were measured using a suitable commercial ELISA Kit (Bay Bioscience Co., Ltd., Hyogo, Japan).

CTL Assay. At 2 weeks after the last immunization, the splenic cells collected from immunized mice were plated in 6-well plates and coincubated with mitomycin C-treated tumor cells (B16BL6 cells, EL4 cells and colon-26 cells) for 4 days. After 4 days of coincubation, nonadherent cells were harvested, washed and plated in 96-well plates with target cells (B16BL6 cells, EL4 cells and colon-26 cells) at various effector cell/target cell (E/T) ratios. The target tumor cells were labeled with ^{51}Cr by incubating with Na$_2$^{51}CrO$_4$ (PerkinElmer, Inc., MA, USA) in culture medium for 1 h at 37 °C. At 4 h after incubation, the plates were centrifuged, and the supernatant in each well was collected and the radioactivity of released ^{51}Cr was measured in a gamma counter. The percentage of ^{51}Cr release was calculated as follows: specific lysis (%) = [(experimental ^{51}Cr release − spontaneous ^{51}Cr release)/ (maximum ^{51}Cr release − spontaneous ^{51}Cr release)] × 100).

Therapeutic Experiments in Solid Tumor Models. At 2 weeks after the last immunization or on the immunization day, B16BL6 cells, EL4 cells and colon-26 cells were transplanted subcutaneously into the back of the mice (1 × 10^6 cells). The tumor size was measured with calipers in two dimensions, and the tumor volume was calculated using the following equation: volume (mm^3) = $\pi/6$ × longer diameter × (shorter diameter)^2. The survival of the mice was monitored up to 100 days after the transplantation of tumor cells.

Therapeutic Experiments in Lung Metastatic Tumor Models. At 2 weeks after the last immunization or on the immunization day, B16BL6 cells or colon-26 cells were intravenously administered via the tail vein (1 × 10^5 cells) and the survival of the mice was monitored up to 100 days after administration of the tumor cells. To evaluate metastasis, B16BL6/Luc cells or colon-26/Luc cells were intravenously administered via the tail vein (1 × 10^5 cells). At 14 days after the administration of the tumor cells, the number of B16BL6/Luc cells and colon-26/Luc cells in the lung was quantitatively evaluated by measuring luciferase activity as previously reported.[36,37]

Statistical Analysis. Results were presented as the mean ± SD of more than three experiments. Analysis of variance (ANOVA) was used to test the statistical significance of differences among groups. Two-group comparisons were performed by the Student's t test. Multiple comparisons between control groups and other groups were performed by the Dunnett's test, and multiple

comparisons between all groups were performed by the Tukey—Kramer test.

RESULTS

Physicochemical Properties of Bubble Lipoplexes Constructed with pUb-M. The physicochemical properties of lipoplexes and bubble lipoplexes constructed with pUb-M used in all experiments were evaluated by measuring the particle sizes and zeta potentials. The mean particle sizes and zeta potentials of nonmodified PEG_{2000}-lipoplexes (Bare-PEG_{2000} lipoplexes) and mannose-conjugated PEG_{2000}-lipoplexes (Man-PEG_{2000} lipoplexes) were 144 ± 13 nm, 45.7 ± 4.5 mV and 143 ± 10 nm, 44.5 ± 5.8 mV, respectively (Table 1). Moreover, the mean particle sizes and zeta potentials of nonmodified bubble lipoplexes (Bare-PEG_{2000} bubble lipoplexes) and Man-PEG_{2000} bubble lipoplexes were 557 ± 20 nm, 46.7 ± 4.2 mV and 555 ± 19 nm, 45.1 ± 2.2 mV, respectively (Table 1). These results corresponded to our previous reports using other pDNA,[33] suggesting that pDNA had no effect on the physicochemical properties of Man-PEG_{2000} bubble lipoplexes.

Splenic Dendritic Cell-Selective and -Efficient Gene Expression by Gene Transfer Using Man-PEG_{2000} Bubble Lipoplexes and US Exposure. First, to investigate the level of gene expression by Man-PEG_{2000} bubble lipoplexes and US exposure in the spleen, we measured the relative mRNA copy numbers of Ub-M after transfection. As shown in Figures 1A and 1B, the level of Ub-M mRNA expression obtained by Man-PEG_{2000} bubble lipoplexes and US exposure reached a peak at 6 h after transfection. Moreover, that level of Ub-M mRNA expression was markedly higher than that obtained by Bare- and Man-PEG_{2000} lipoplexes, and significantly higher than that obtained by Bare-PEG_{2000} bubble lipoplexes and US exposure. Then, we investigated the mannose receptor-expressing cell selectivity of Ub-M mRNA expression obtained by gene transfer using Man-PEG_{2000} bubble lipoplexes and US exposure. In the spleen, the relative mRNA copy numbers of Ub-M in $CD11c^+$ cells was significantly higher than that in $CD11c^-$ cells following transfection using Man-PEG_{2000} bubble lipoplexes and US exposure (Figure 1C). On the other hand, no selective gene expression in $CD11c^+$ cells was observed by gene transfer using Bare-PEG_{2000} bubble lipoplexes and US exposure (Figure 1C).

Antigen-Stimulatory Th1 Cytokine Secretion from the Splenic Cells Immunized by Man-PEG_{2000} Bubble Lipoplexes and US Exposure. To evaluate the melanoma-specific cytokine secretion from immunized splenic cells, splenic cells immunized by pUb-M were incubated with each tumor cell-lysate in vitro, and then, Th1 and Th2 cytokines secreted in the supernatants were measured. Following investigation of the expression level of gp100 and TRP-2, a melanoma-specific antigen, in each cell used in this study, the expression of gp100 and TRP-2 was only detected in B16BL6 cells which are melanoma cell lines (Supplementary Figure 1 in the Supporting Information). As results of the immunization according to the protocol shown in Figure 2A, the splenic cells immunized by Man-PEG_{2000} bubble lipoplexes and US exposure secreted the highest amount of IFN-γ and TNF-α, which are Th1 cytokines, in the presence of B16BL6 cell lysates (Figures 2B and 2C). On the other hand, the secretion of Th1 cytokines (IFN-γ and TNF-α) was lower in all the groups in the presence of EL4 and colon-26 cell lysates. Moreover, the secretion of IL-4 and IL-6, which are Th2 cytokines, was also lower in all the groups in the presence of each cell lysate (Figures 2D and 2E). These observations suggest that pUb-M transfer by
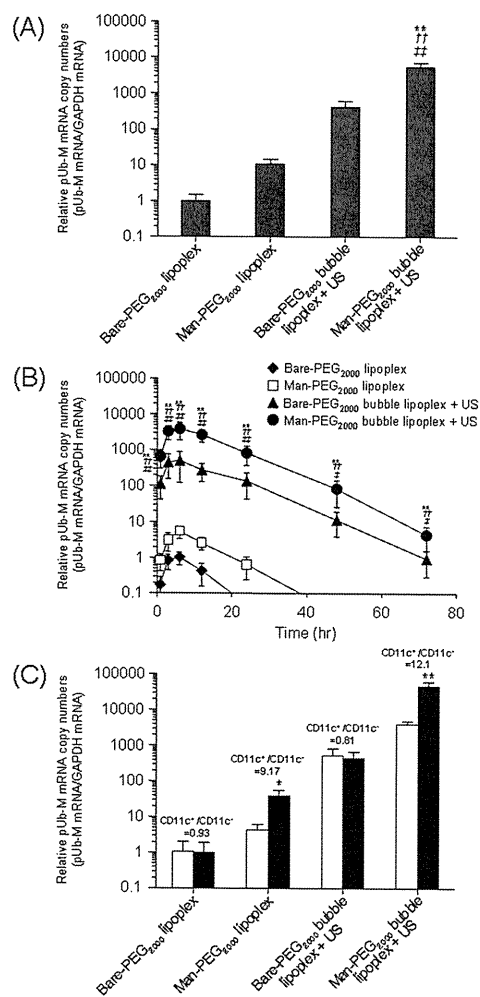

Figure 1. Enhanced Ub-M mRNA expression in the spleen and the splenic dendritic cells ($CD11c^+$ cells) by Man-PEG_{2000} bubble lipoplexes constructed with pUb-M and US exposure in vivo. (A) The level of Ub-M mRNA expression obtained by Bare-PEG_{2000} lipoplexes, Man-PEG_{2000} lipoplexes, Bare-PEG_{2000} bubble lipoplexes with US exposure and Man-PEG_{2000} bubble lipoplexes with US exposure (50 μg of pDNA) in the spleen at 6 h after transfection. Each value represents the mean + SD (n = 4). $^{**}p < 0.01$, compared with Bare-PEG_{2000} lipoplex; $^{\dagger\dagger}p < 0.01$, compared with Man-$PEG_{2000}$ lipoplex; $^{\ddagger\ddagger}p < 0.01$, compared with Bare-$PEG_{2000}$ bubble lipoplex + US. (B) Time-course of Ub-M mRNA expression in the spleen after transfection by Bare-PEG_{2000} lipoplexes, Man-PEG_{2000} lipoplexes, Bare-PEG_{2000} bubble lipoplexes with US exposure and Man-PEG_{2000} bubble lipoplexes with US exposure (50 μg of pDNA). Each value represents the mean $\pm$ SD (n = 4). $^{**}p < 0.01$, compared with the corresponding group of Bare-PEG_{2000} lipoplex; $^{\dagger\dagger}p < 0.01$, compared with the corresponding group of Man-PEG_{2000} lipoplex; $^{\ddagger}p < 0.05$; $^{\ddagger\ddagger}p < 0.01$, compared with the corresponding group of Bare-PEG_{2000} bubble lipoplex + US. (C) Splenic cellular localization of Ub-M mRNA expression at 6 h after transfection by Bare-PEG_{2000} lipoplexes, Man-PEG_{2000} lipoplexes, Bare-PEG_{2000} bubble lipoplexes with US exposure and Man-PEG_{2000} bubble lipoplexes with US exposure (50 μg of pDNA). Each value represents the mean + SD (n = 4). $^*p < 0.05$; $^{**}p < 0.01$, compared with the corresponding group of $CD11c^-$ cells.

Man-PEG_{2000} bubble lipoplexes and US exposure significantly enhances the differentiation of helper T cells into Th1.

Induction of Melanoma-Specific CTLs by pUb-M Transfer Using Man-PEG_{2000} Bubble Lipoplexes and US Exposure. We investigated the melanoma-specific CTL activities in the
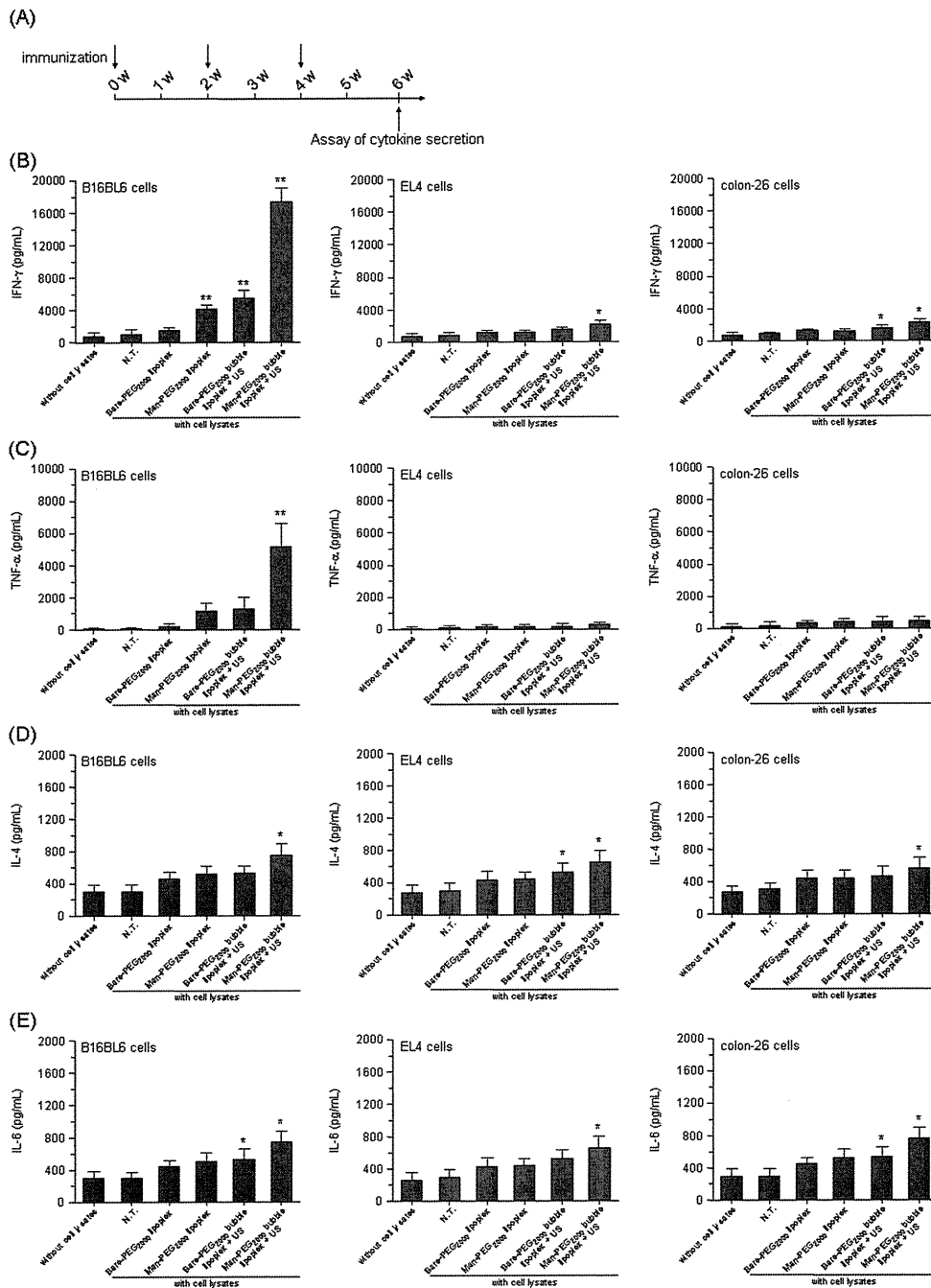
Figure 2. Melanoma-stimulatory cytokine secretion characteristics by DNA vaccination using Man-PEG$_{2000}$ bubble lipoplexes constructed with pUb-M and US exposure. (A) Schedule of immunization for the evaluation of melanoma-stimulatory cytokine secretion characteristics. (B—E) Each cancer cell lysate-specific IFN-γ (B), TNF-α (C), IL-4 (D) and IL-6 (E) secretion from the splenic cells immunized three times biweekly with Bare-PEG$_{2000}$ lipoplexes, Man-PEG$_{2000}$ lipoplexes, Bare-PEG$_{2000}$ bubble lipoplexes with US exposure and Man-PEG$_{2000}$ bubble lipoplexes with US exposure (50 μg of pDNA). The splenic cells were collected at 2 weeks after the last immunization. After the immunized splenic cells were cultured for 72 h in the presence of each cancer cell lysate (100 μg protein), IFN-γ, TNF-α, IL-4 and IL-6 secreted in the medium were measured by ELISA. Each value represents the mean + SD ($n = 4$). *$p < 0.05$; **$p < 0.01$, compared with the corresponding "without cell lysate" group.

splenic cells immunized by pUb-M. This experiment was performed according to the protocol shown in Figure 3A. As shown in Figure 3B, the splenic cells immunized by Man-PEG$_{2000}$ bubble lipoplexes and US exposure showed the highest CTL activities of all groups stimulated by B16BL6 cells. In contrast, no CTL activity was obtained in all groups stimulated by EL4 and colon-26 cells (Figures 3C and 3D). These results suggest that melanoma-specific CTLs are induced effectively in the splenic

cells transfected pUb-M by Man-PEG$_{2000}$ bubble lipoplexes and US exposure.

Cancer Vaccine Effects against Melanoma-Derived Solid and Metastatic Tumors by DNA Vaccination Using Man-PEG$_{2000}$ Bubble Lipoplexes and US Exposure. Cancer vaccine effects against solid and metastatic tumors obtained by DNA vaccination using Man-PEG$_{2000}$ lipoplexes and US exposure were examined. First, we evaluated the level of gp100 and
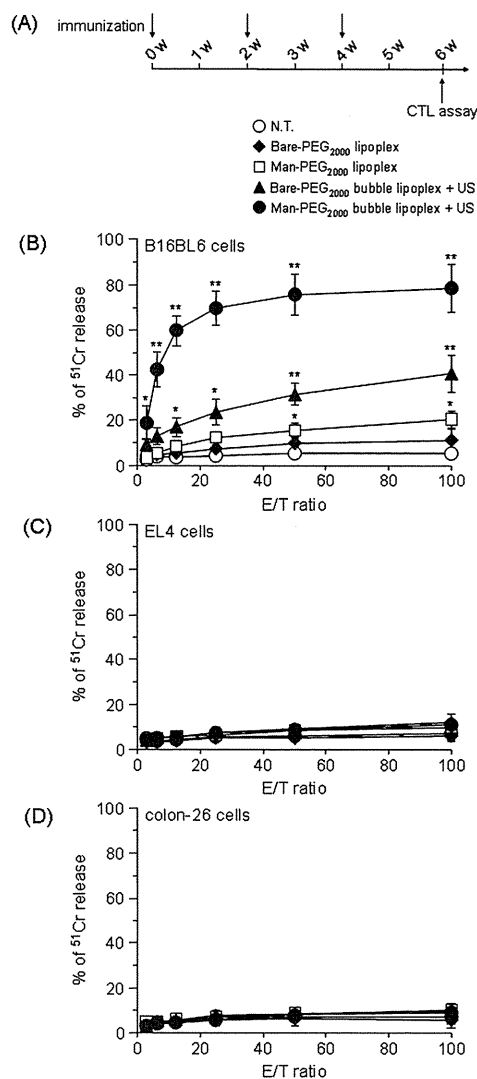
Figure 3. Evaluation of melanoma-specific CTL activities by DNA vaccination using Man-PEG$_{2000}$ bubble lipoplexes and US exposure. (A) Schedule of immunization for the assay of melanoma-specific CTL activities. (B−D) Each cancer cell lysate-specific CTL activities after immunization three times with Bare-PEG$_{2000}$ lipoplexes, Man-PEG$_{2000}$ lipoplexes, Bare-PEG$_{2000}$ bubble lipoplexes with US exposure and Man-PEG$_{2000}$ bubble lipoplexes with US exposure (50 μg of pDNA). The splenic cells were collected at 2 weeks after the last immunization, and then, the splenic cells were coincubated with ^{51}Cr-labeled cancer cells. CTL activities against B16BL6 cells (B), EL4 cells (C) and colon-26 cells (D) in the immunized splenic cells were determined by ^{51}Cr release assay. Each value represents the mean ± SD (n = 4). *p < 0.05; **p < 0.01, compared with the corresponding "N.T." (no treatment) group.

TRP-2 expression in each tumor used in this study, and confirmed that the expression of gp100 and TRP-2 was only detected in B16BL6 tumor (Supplementary Figure 2 in the Supporting Information). Following investigation of cancer vaccine effects against solid tumors according to the protocol shown in Figure 4A, B16BL6-transplanted tumor growth was significantly suppressed in mice immunized with Man-PEG$_{2000}$ bubble lipoplexes constructed with pUb-M and US exposure (Figures 4B and 4D). Moreover, the survival of B16BL6-transplanted mice was significantly prolonged by DNA vaccination using Man-PEG$_{2000}$ bubble lipoplexes constructed with pUb-M and US exposure, and complete tumor-rejection was observed in 7/10 of

B16BL6-transplanted mice (Figure 4C). These vaccine effects were obtained against B16F1-transplanted mice (Supplementary Figure 4B in the Supporting Information); on the other hand, no cancer vaccine effects against EL4 and colon-26 cell-derived tumors, which do not express gp100 and TRP-2, were observed in all groups (Figures 4B−D). In addition, these DNA vaccine effects against B16BL6-derived tumors were not observed in mice immunized by Man-PEG$_{2000}$ bubble lipoplexes constructed with pcDNA3.1 (control vector) and US exposure (Supplementary Figure 3 in the Supporting Information), suggesting that DNA vaccine effects against melanoma are attributed to not pDNA transfer itself but melanoma-related antigens expressed by pUb-M.

Then, we investigated the cancer vaccine effects against a pulmonary metastatic tumor obtained by DNA vaccination using Man-PEG$_{2000}$ bubble lipoplexes and US exposure. Following experiments according to the protocol shown in Figure 5A, the level of luciferase expression derived from B16BL6/Luc cells in the lung, which express gp100 and TRP-2 (Supplementary Figures 1 and 2 in the Supporting Information), was significantly suppressed in mice immunized by Man-PEG$_{2000}$ bubble lipoplexes and US exposure (Figures 5B and 5D). Moreover, the survival of the pulmonary metastatic tumor model mice constructed with B16BL6 cells was significantly prolonged by DNA vaccination using Man-PEG$_{2000}$ bubble lipoplexes and US exposure (Figure 5C). These vaccine effects were obtained against pulmonary metastatic B16F1-derived tumor model mice (Supplementary Figure 4C in the Supporting Information); on the other hand, no therapeutic effects against colon-26 cells by DNA vaccination using this method were observed in any of the groups (Figures 5B−D).

Effect of Administration Routes of Man-PEG$_{2000}$ Bubble Lipoplexes on Cancer Vaccine Effects. Next, we evaluated the effects of the administration routes of Man-PEG$_{2000}$ bubble lipoplexes to obtain effective DNA vaccine effects. In this experiment, in addition to pUb-M transfer using intravenous administration of Man-PEG$_{2000}$ bubble lipoplexes and external US exposure, we investigated the DNA vaccine effects by pUb-M transfer using intradermal and intrasplenic administration of Man-PEG$_{2000}$ bubble lipoplexes and direct US exposure to the administration sites. In the preliminary experiments about US intensity for obtaining the highest gene expression in the spleen and skin, the optimized intensities of US exposure to the abdominal area by a probe of diameter 20 mm and to the injected sites directly by a probe of diameter 6 mm are 1.0 W/cm^2 and 4.0 W/cm^2, respectively (data not shown). Based on these investigations, we used the different US intensity depending on the probe size and US-exposed sites in this study. Following immunization against melanoma according to the protocol shown in Figure 6A, B16BL6-transplanted tumor growth was suppressed the best in mice transfected with pUb-M using intravenous injection of Man-PEG$_{2000}$ bubble lipoplexes and external US exposure (Figure 6B). Moreover, the survival of B16BL6-transplanted mice was also prolonged the best by DNA vaccination using intravenous injection of Man-PEG$_{2000}$ bubble lipoplexes and external US exposure (Figure 6C).

Duration of DNA Vaccine Effects by Man-PEG$_{2000}$ Bubble Lipoplexes and US Exposure. Finally, to investigate the duration of DNA vaccine effects following pUb-M transfer using Man-PEG$_{2000}$ bubble lipoplexes and US exposure, B16BL6 cells were retransplanted in mice in which first-transplanted tumors derived from B16BL6 cells were completely rejected by DNA
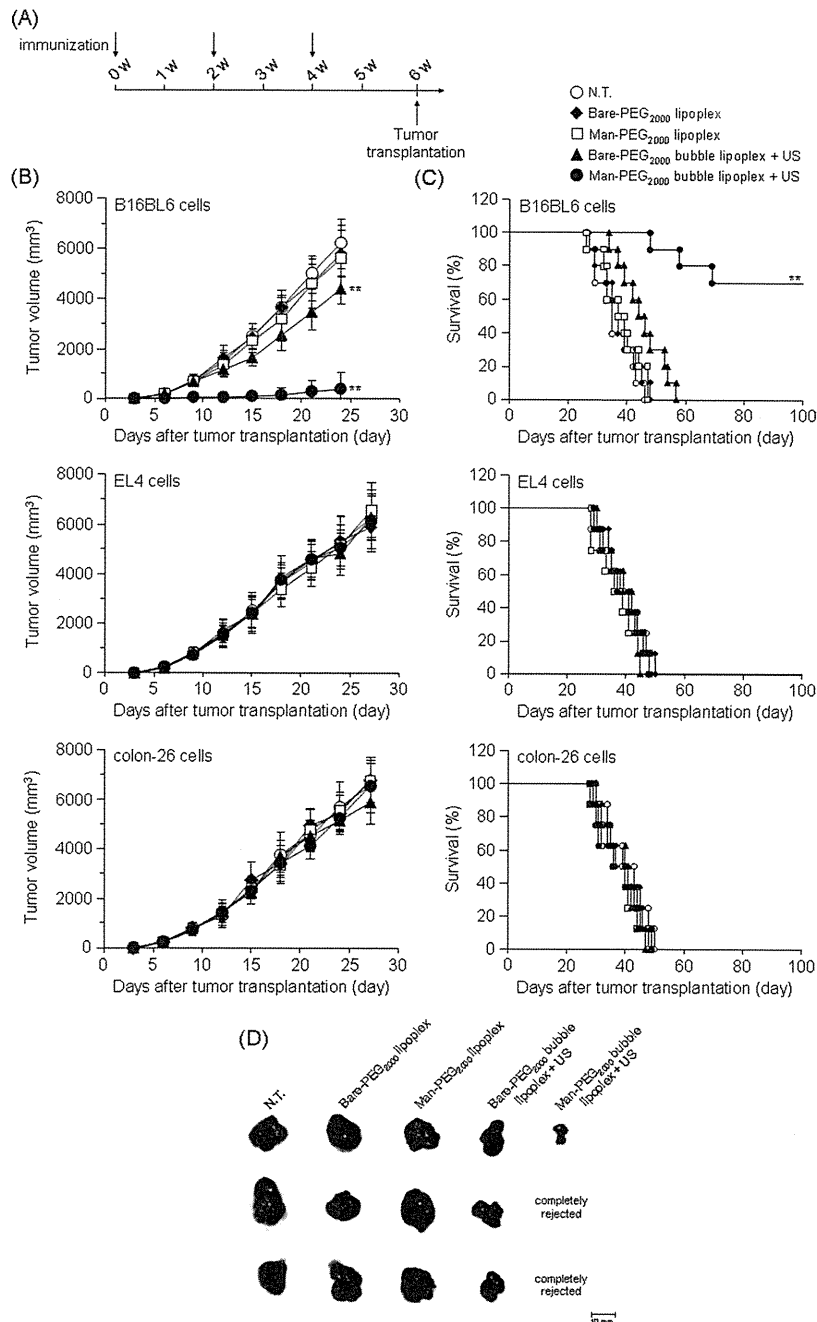
Figure 4. Cancer vaccine effects against solid tumors by DNA vaccination using Man-PEG$_{2000}$ bubble lipoplexes and US exposure. (A) Schedule of therapeutic experiments on solid tumors. (B, C) The suppressing effects of tumor growth against solid tumors (B) and the prolonging effects of survival in tumor-transplanted mice (C) by DNA vaccination using Bare-PEG$_{2000}$ lipoplexes, Man-PEG$_{2000}$ lipoplexes, Bare-PEG$_{2000}$ bubble lipoplexes with US exposure and Man-PEG$_{2000}$ bubble lipoplexes with US exposure (50 μg of pDNA). Two weeks after the last immunization, B16BL6 cells, EL4 cells and colon-26 cells (1 × 10^6 cells) were transplanted subcutaneously into the back of mice (n = 8−10). The tumor volume was evaluated (each value represents the mean ± SD), and the survival was monitored up to 100 days after the tumor transplantation. $**p < 0.01$, compared with the corresponding "N.T." (no treatment) group. (D) Photograph of a B16BL6 cell-derived solid tumor at 15 days after the tumor transplantation in mice immunized by each transfection method (n = 3).

vaccination using Man-PEG$_{2000}$ bubble lipoplexes and US exposure at 100 days after the first transplantation (Figure 7A). As shown in Figure 7B, compared with N.T. mice, the second-transplanted tumor growth derived from B16BL6 cells was markedly suppressed and the survival of B16BL6-transplanted mice was significantly prolonged. In addition, we also evaluated the duration of DNA vaccine effects against a pulmonary metastatic tumor. Following intravenous injection of B16BL6/Luc cells into

mice at 100 days after the last immunization (Figure 7C), the level of luciferase expression derived from B16BL6/Luc cells in the lung was significantly suppressed and the survival of pulmonary metastatic tumor model mice constructed with B16BL6 cells was significantly prolonged in mice transfected with pUb-M using Man-PEG$_{2000}$ bubble lipoplexes and US exposure (Figure 7D). These results suggest that DNA vaccine effects by pUb-M transfer using Man-PEG$_{2000}$ bubble lipoplexes and US exposure
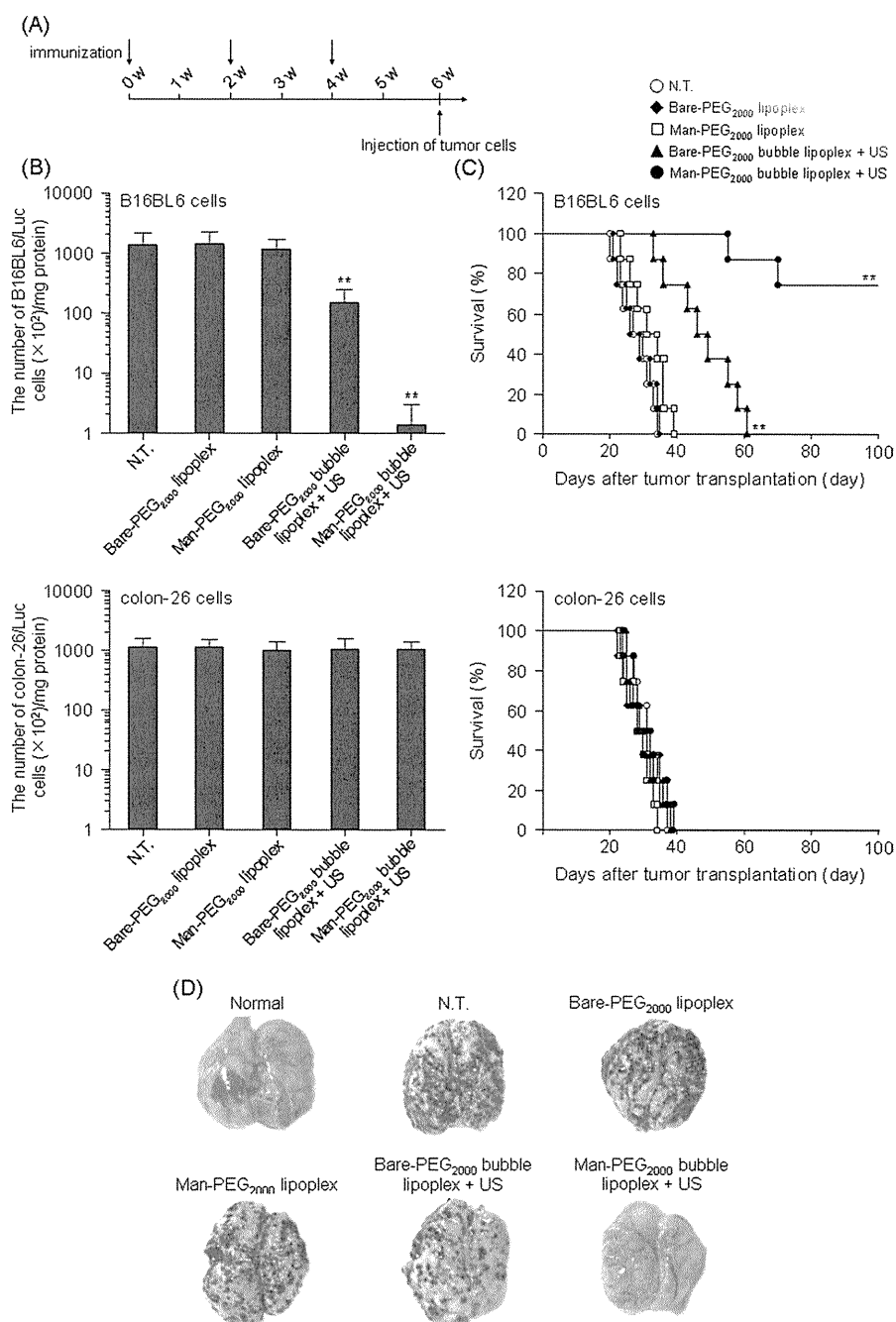
Figure 5. Cancer vaccine effects against pulmonary metastatic tumors by DNA vaccination using Man-PEG$_{2000}$ bubble lipoplexes and US exposure. (A) Schedule of therapeutic experiments involving pulmonary metastatic tumors. (B, C) The suppressing effects of pulmonary metastatic tumors (B) and the prolonging of survival (C) by DNA vaccination using Bare-PEG$_{2000}$ lipoplexes, Man-PEG$_{2000}$ lipoplexes, Bare-PEG$_{2000}$ bubble lipoplexes with US exposure and Man-PEG$_{2000}$ bubble lipoplexes with US exposure (50 μg of pDNA). Two weeks after the last immunization, B16BL6/Luc and colon-26/ Luc cells (for the evaluation of tumor metastasis) and B16BL6 and colon-26 cells (for the evaluation of survival) were injected intravenously (1×10^5 cells) into mice. The pulmonary metastatic tumors at 14 days after the tumor injection were evaluated by the luciferase activity ($n = 5$, each value represents the mean ± SD), and the survival was monitored up to 100 days after the tumor injection ($n = 8$). $**p < 0.01$, compared with the corresponding "N.T." (no treatment) group. (D) Photograph of a B16BL6-derived pulmonary metastatic tumor at 14 days after the tumor injection in mice immunized by each transfection method.

were sustained for at least 100 days against both solid and metastatic tumors.

■ DISCUSSION

The prognosis is poor for patients with melanoma, who exhibit a high rate of metastasis and relapse; therefore, the development

of therapy for suppressing this melanoma metastasis and relapse is required.[2,3] It has been reported that DNA vaccination is effective for the prevention of metastasis and relapse,[5,7,8] and especially the application of DNA vaccination against melanoma has been focused since the identification of cancer antigens such as gp100, MART-1 and TRP is proceeding in melanoma.[10–13]
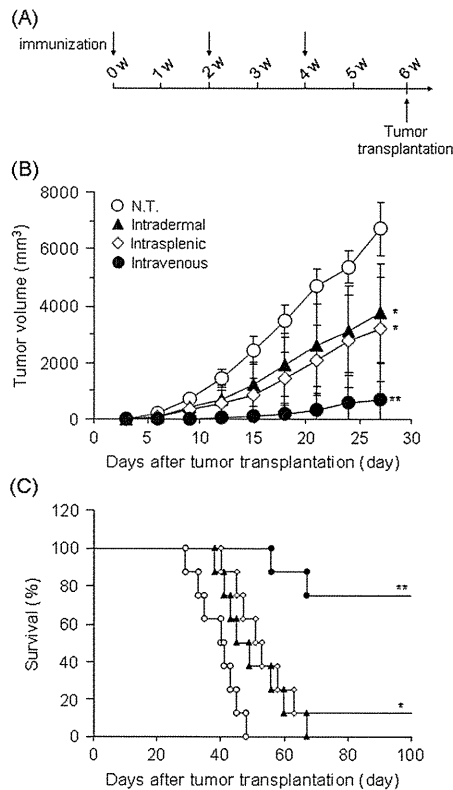
Figure 6. Effects of administration routes of Man-PEG$_{2000}$ bubble lipoplexes on DNA vaccine effects. (A) Schedule of therapeutic experiments. (B, C) The suppressing effects of tumor growth against solid tumors (B) and the prolonging of survival in tumor-transplanted mice (C) by DNA vaccination using various administration routes of Man-PEG$_{2000}$ bubble lipoplexes (50 μg of pDNA) and US exposure. Man-PEG$_{2000}$ bubble lipoplexes were given by intradermal, intrasplenic and intravenous administration into mice, and US was exposed to the injected site directly or to the abdominal area externally. Two weeks after the last immunization, B16BL6 cells (1 × 10^6 cells) were transplanted subcutaneously into the back of mice (n = 8). The tumor volume was evaluated (each value represents the mean ± SD), and the survival was monitored up to 100 days after the tumor transplantation. *p < 0.05; **p < 0.01, compared with the corresponding "N.T." (no treatment) group.

Figure 7. Duration of DNA vaccine effects by Man-PEG$_{2000}$ bubble lipoplexes and US exposure. (A) Schedule of therapeutic experiments against solid tumors. At 100 days after first transplantation of B16BL6 cells into mice immunized three times by Man-PEG$_{2000}$ bubble lipoplexes and US exposure, B16BL6 cells (1 × 10^6 cells) were retransplanted subcutaneously into the back of mice who completely rejected the first transplanted tumors (n = 7). (B) The suppressing effects of tumor growth against solid tumors and the prolonging of survival in tumor-transplanted mice by DNA vaccination using Man-PEG$_{2000}$ bubble lipoplexes and US exposure (50 μg of pDNA). The tumor volume was evaluated (each value represents the mean ± SD), and the survival was monitored up to 100 days after the tumor retransplantation. (C) Schedule of therapeutic experiments against metastatic tumors. At 100 days after the last immunization using Bare-PEG$_{2000}$ lipoplexes, Man-PEG$_{2000}$ lipoplexes, Bare-PEG$_{2000}$ bubble lipoplexes with US exposure and Man-PEG$_{2000}$ bubble lipoplexes with US exposure (50 μg of pDNA), B16BL6 cells (for the evaluation of tumor metastasis) and B16BL6 cells (for the evaluation of survival days) were injected intravenously (1 × 10^5 cells) into mice. (D) The suppressing effects of B16BL6 cell-derived pulmonary metastatic tumors and the prolonging of survival by DNA vaccination using Bare-PEG$_{2000}$ lipoplexes, Man-PEG$_{2000}$ lipoplexes, Bare-PEG$_{2000}$ bubble lipoplexes with US exposure and Man-PEG$_{2000}$ bubble lipoplexes with US exposure (50 μg of pDNA). The pulmonary metastatic tumors at 14 days after the injection of B16BL6 cells were evaluated by the luciferase activity (n = 4), and the survival was monitored up to 100 days (n = 8). **p < 0.01, compared with the corresponding "N.T." (no treatment) group.

On the other hand, it is essential to transfer effectively into APCs such as dendritic cells to obtain potent therapeutic effects by DNA vaccination.[14,15] In the present study, we applied an APC-selective and -efficient gene transfection method using Man-PEG$_{2000}$ bubble lipoplexes constructed with gp100 and TRP-2-encoding pDNA and US exposure to DNA vaccination against melanoma with metastatic and relapsed properties.

The delivery of antigen-encoding gene into the dendritic cells, known as a major target cells for cancer immunotherapy, is necessary to achieve potent therapeutic effects with DNA vaccination.[14,15] However, it seems that the number of dendritic cells distributed in organs, such as spleen and skin, is low for DNA vaccination.[38] Moreover, gene transfection efficiency in dendritic cells is low,[20] because dendritic cells are poorly dividing cells[39,40] and immune effector cells are highly sensitive to cationic lipids.[41] To overcome these obstacles, gene transfection methods using external physical stimulation, such as electropolation, hydrodynamic injection and sonoporation, have been investigated for cancer vaccination.[21−25] In particular, sonoporation methods using microbubbles and US exposure are expected to be suitable
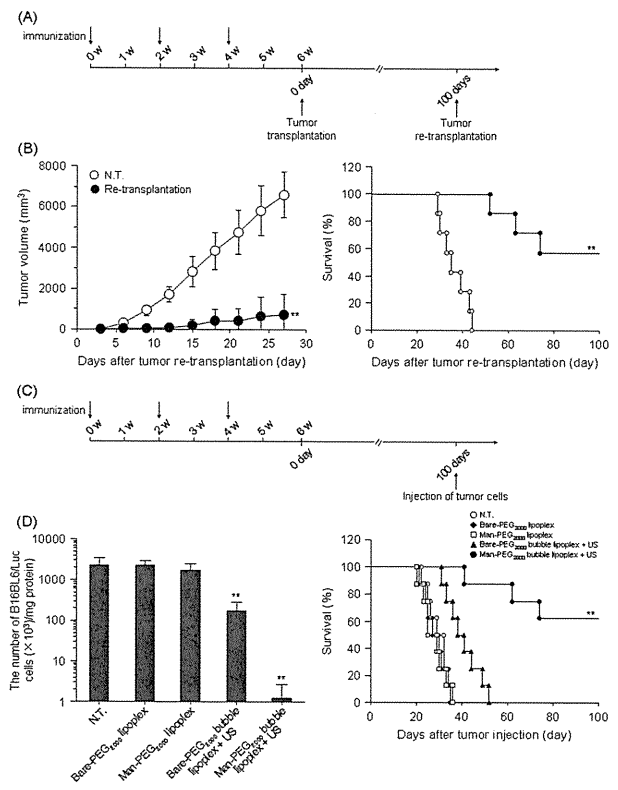
as a gene transfection method for DNA vaccination in clinical situation, because microbubbles and US exposure systems have been used for diagnostic imaging[42,43] and calculus fragmentation[44,45] in clinical situation. We have developed a gene transfection method using Man-PEG$_{2000}$ bubble lipoplexes and US exposure, and succeeded in obtaining APC-selective and -efficient gene expression following experiments using luciferase-encoding pDNA.[33] In this study using pUb-M which expresses melanoma-related antigens (gp100 and TRP-2), a high level of expression in

the spleen was obtained by gene transfer using intravenous injection of Man-PEG$_{2000}$ bubble lipoplexes and external US exposure (Figures 1A and 1B). Moreover, this gene expression was obtained selectively in the splenic CD11c$^+$ cells, known as dendritic cells[46] (Figure 1C), and these findings corresponded to those in our previous reports of using firefly luciferase-encoding pDNA.[33] In our previous report using pCMV-Luc and pCMV-OVA, we showed that the enhanced gene expression in the spleen was obtained by gene transfer using Man-PEG$_{2000}$ bubble lipoplexes and US exposure, and not observed in gene transfer using Man-PEG$_{2000}$ lipoplexes or Man-PEG$_{2000}$ bubble lipoplexes only and Man-PEG$_{2000}$ lipoplexes with US exposure.[33] These observations suggest that splenic dendritic cell-selective and -efficient expression of melanoma-related antigens can be specifically obtained by the gene transfer using Man-PEG$_{2000}$ bubble lipoplexes constructed with pUb-M and US exposure.

To achieve potent therapeutic effects by DNA vaccination against cancer, the activation of Th1 immunity and the effective induction of CTLs with high antitumor activities are important.[47] The antigen presentation on MHC class I molecules is essential for efficient CTL induction.[6,8,9] Antigens function as endogenous antigens since the cancer antigens are expressed intracellularly in DNA vaccination; consequently, the antigens are presented on MHC class I molecules.[8] As shown in Figure 2, the enhanced secretion of Th1 cytokines (IFN-γ and TNF-α) was observed in the splenic cells immunized by Man-PEG$_{2000}$ bubble lipoplexes constructed with pUb-M and US exposure by addition of B16BL6 cell lysates, compared with that of Th2 cytokines (IL-4 and IL-6). Moreover, the effective induction of CTLs against B16BL6 cells was also observed by DNA vaccination using Man-PEG$_{2000}$ bubble lipoplexes and US exposure (Figure 3). Recently, we have reported that the antigen presentation on MHC class I molecules was also observed in DNA vaccination using Man-PEG$_{2000}$ bubble lipoplexes constructed with OVA-encoding pDNA.[33] These results suggest that antigen presentation of melanoma antigens on MHC class I molecules is responsible for the enhanced secretion of Th1 cytokines stimulated by B16BL6 cell and the induction of CTLs against B16BL6 cells in this study. As shown in Figure 4, the growth of B16BL6 cell-derived tumors was suppressed and the survival of B16BL6 cell-transplanted mice was prolonged by DNA vaccination using Man-PEG$_{2000}$ bubble lipoplexes and US exposure. Since the prognosis of patients with melanoma is poor, because of the high metastatic properties of melanoma as mentioned above,[2,3] we also investigated the vaccine effects against metastatic melanoma by DNA vaccination using this method. As shown in Figure 5, B16BL6 cell-derived pulmonary metastasis constructed by intravenous injection of tumor cells was suppressed by DNA vaccination using this gene transfection method. These DNA vaccine effects followed by Man-PEG$_{2000}$ bubble lipoplexes constructed with pUb-M and US exposure were obtained against not only B16BL6 cells but also B16F1-derived tumors (Supplementary Figure 4 in the Supporting Information), suggesting that this DNA vaccination might be potent against various types of melanoma. On the other hand, the potent therapeutic effects against B16BL6-derived solid and metastatic tumor transplanted mice were not observed in DNA vaccination using Man-PEG$_{2000}$ bubble lipoplexes constructed with pUb-M and US exposure (data not shown). These findings suggest that the optimized duration for immunization is essential for obtaining potent antitumor effects by DNA vaccination using Man-PEG$_{2000}$ bubble lipoplexes and US exposure, and DNA vaccination using Man-PEG$_{2000}$ bubble lipoplexes and US

exposure may be suitable for the prevention of cancer metastasis and relapse. In addition, these vaccine effects against solid and metastatic tumors were sustained for at least 100 days (Figure 7). These observations lead us to believe that the enhanced secretion of Th1 cytokines and the induction of B16BL6 cell-specific CTLs contribute to the effective and long-term DNA vaccine effects against solid and metastatic tumors, following pUb-M transfer into splenic dendritic cells using Man-PEG$_{2000}$ bubble lipoplexes and US exposure.

Intradermal and intrasplenic routes are widely used to transfer pDNA into the Langerhans cells known as dendritic cells in the skin or splenic dendritic cells.[48,49] On the other hand, we obtained potent therapeutic effects by DNA vaccination using intravenous administration of Man-PEG$_{2000}$ bubble lipoplexes and external US exposure in this study. As shown in Figure 6, the DNA vaccine effects obtained by immunization using intravenous administration of Man-PEG$_{2000}$ bubble lipoplexes were higher, compared with that using intradermal and intrasplenic administration. In the gene transfer using intradermal/intrasplenic administration of Man-PEG$_{2000}$ bubble lipoplexes, it is assumed that the diffusibility of Man-PEG$_{2000}$ bubble lipoplexes is not good and the delivering efficiency to the dendritic cells may be low, because of the large particle size of Man-PEG$_{2000}$ bubble lipoplexes (approximately 500 nm (Table 1)). Therefore, it may be difficult to deliver the antigen-encoding pDNA into a large number of dendritic cells in the gene transfection process using intradermal/intrasplenic administration of Man-PEG$_{2000}$ bubble lipoplexes. On the other hand, when Man-PEG$_{2000}$ bubble lipoplexes were administered intravenously, the antigen-encoding pDNA may be delivered into a large number of dendritic cells widely distributed in the spleen through the blood vessels. Therefore, it is assumed that potent vaccine effects are obtained by gene transfer in the dendritic cells widely distributed in the spleen. These results suggest that the intravenous administration of Man-PEG$_{2000}$ bubble lipoplexes is suitable to obtain high therapeutic effects by DNA vaccination using Man-PEG$_{2000}$ bubble lipoplexes and US exposure.

In this study, melanoma-specific vaccine effects were induced by DNA vaccination using Man-PEG$_{2000}$ bubble lipoplexes and US exposure, and moreover, intravenous administration of ManPEG$_{2000}$ bubble lipoplexes was found to be suitable for DNA vaccination using this method in mice (Figure 6). For clinical application to achieve efficient DNA vaccination, Man-PEG$_{2000}$ bubble lipoplexes need to be delivered to the spleen efficiently at a low dose. Recently, a medical catheter, which possesses a device to inject the microbubbles and to expose US, has been developed for the treatment of thrombolysis in clinical situation.[44,45] During treatment, this catheter is positioned within the lesion sites via the vessels, and various types of drugs, such as the lytic agents and microbubbles, are infused simultaneously with US exposure. Since this system may enable the local injection of Man-PEG$_{2000}$ bubble lipoplexes and direct US exposure to the spleen by catheter delivery via the blood vessels, more potent DNA vaccine effects against melanoma are expected to be obtained at a low dose of Man-PEG$_{2000}$ bubble lipoplexes by applying this catheter-based US system in the future.

■ CONCLUSION

In the present study, we developed DNA vaccination using Man-PEG$_{2000}$ bubble lipoplexes constructed with pUb-M encoding ubiquitylated melanoma-specific antigens (gp100 and TRP-2) and US exposure, and succeeded in obtaining potent DNA vaccine effects against solid and metastatic cancers derived from B16BL6

ARTICLE

melanoma specifically. Moreover, its vaccine effects against melanoma were sustained for 100 days at least. The findings obtained in this study suggest that the gene transfection method using Man-PEG$_{2000}$ bubble lipoplexes and US exposure could be suitable for DNA vaccination aimed at the prevention of metastatic and relapsed cancer.

■ ASSOCIATED CONTENT

⑤ Supporting Information. Additional figures as discussed in the text. This material is available free of charge via the Internet at http://pubs.acs.org.

■ AUTHOR INFORMATION

Corresponding Author
*Department of Drug Delivery Research, Graduate School of Pharmaceutical Sciences, Kyoto University, 46-29 Yoshida-shimoadachi-cho, Sakyo-ku, Kyoto 606-8501, Japan. Phone: +81-75-753-4545. Fax: +81-75-753-4575. E-mail: hashidam@pharm.kyoto-u.ac.jp (M.H.), kawakami@pharm.kyoto-u.ac.jp (S.K.).

■ ACKNOWLEDGMENT

■ REFERENCES

(1) Welch, H. G.; Woloshin, S.; Schwartz, L. M. Skin biopsy rates and incidence of melanoma: population based ecological study. *BMJ* 2005, *331*, 481.

(2) Mocellin, S.; Hoon, D.; Ambrosi, A.; Nitti, D.; Rossi, C. R. The prognostic value of circulating tumor cells in patients with melanoma: a systematic review and meta-analysis. *Clin. Cancer Res.* 2006, *12*, 4605–4613.

(3) Francken, A. B.; Accortt, N. A.; Shaw, H. M.; Wiener, M.; Soong, S. J.; Hoekstra, H. J.; Thompson, J. F. Prognosis and determinants of outcome following locoregional or distant recurrence in patients with cutaneous melanoma. *Ann. Surg. Oncol.* 2008, *15*, 1476–1484.

(4) Begley, J.; Ribas, A. Targeted therapies to improve tumor immunotherapy. *Clin. Cancer Res.* 2008, *14*, 4385–4391.

(5) Jandus, C.; Speiser, D.; Romero, P. Recent advances and hurdles in melanoma immunotherapy. *Pigm. Cell Melanoma Res.* 2009, *22*, 711–723.

(6) Donnelly, J. J.; Wahren, B.; Liu, M. A. DNA vaccines: progress and challenges. *J. Immunol.* 2005, *175*, 633–639.

(7) Terando, A. M.; Faries, M. B.; Morton, D. L. Vaccine therapy for melanoma: current status and future directions. *Vaccine* 2007, *25S*, B4–16.

(8) Kutzler, M. A.; Weiner, D. B. DNA vaccines: ready for prime time?. *Nat. Rev. Genet.* 2008, *9*, 776–788.

(9) Rice, J.; Ottensmeier, C. H.; Stevenson, F. K. DNA vaccines: precision tools for activating effective immunity against cancer. *Nat. Rev. Cancer* 2008, *8*, 108–120.

(10) Bloom, M. B.; Perry-Lalley, D.; Robbins, P. F.; Li, Y.; el-Gamil, M.; Rosenberg, S. A.; Yang, J. C. Identification of tyrosinase-related protein 2 as a tumor rejection antigen for the B16 melanoma. *J. Exp. Med.* 1997, *185*, 453–459.

(11) de Vries, T. J.; Fourkour, A.; Wobbes, T.; Verkroost, G.; Ruiter, D. J.; van Muijen, G. N. Heterogeneous expression of immunotherapy candidate proteins gp100, MART-1, and tyrosinase in human melanoma cell lines and in human melanocytic lesions. *Cancer Res.* 1997, *57*, 3223–3229.

(12) Urosevic, M.; Braun, B. Willers, J.; Burg, G.; Dummer, R. Expression of melanoma-associated antigens in melanoma cell cultures. *Exp. Dermatol.* 2005, *14*, 491–497.

(13) Yuan, J.; Ku, G. Y.; Gallardo, H. F.; Orlandi, F.; Manukian, G.; Rasalan, T. S.; Xu, Y.; Li, H.; Vyas, S.; Mu, Z.; Chapman, P. B.; Krown, S. E.; Panageas, K.; Terzulli, S. L.; Old, L. J.; Houghton, A. N.; Wolchok, J. D. Safety and immunogenicity of a human and mouse gp100 DNA vaccine in a phase I trial of patients with melanoma. *Cancer Immun.* 2009, *9*, 5.

(14) Chattergoon, M. A.; Robinson, T. M.; Boyer, J. D.; Weiner, D. B. Specific immune induction following DNA-based immunization through in vivo transfection and activation of macrophages/antigen-presenting cells. *J. Immunol.* 1998, *160*, 5707–5718.

(15) Melief, C. J. Cancer immunotherapy by dendritic cells. *Immunity* 2008, *29*, 372–383.

(16) Hattori, Y.; Suzuki, S.; Kawakami, S.; Yamashita, F.; Hashida, M. The role of dioleoylphosphatidylethanolamine (DOPE) in targeted gene delivery with mannosylated cationic liposomes via intravenous route. *J. Controlled Release* 2005, *108*, 484–495.

(17) Hattori, Y.; Kawakami, S.; Nakamura, K.; Yamashita, F.; Hashida, M. Efficient gene transfer into macrophages and dendritic cells by in vivo gene delivery with mannosylated lipoplex via the intraperitoneal route. *J. Pharmacol. Exp. Ther.* 2006, *318*, 828–834.

(18) Hattori, Y.; Kawakami, S.; Lu, Y.; Nakamura, K.; Yamashita, F.; Hashida, M. Enhanced DNA vaccine potency by mannosylated lipoplex after intraperitoneal administration. *J. Gene Med.* 2006, *8*, 824–834.

(19) Lu, Y.; Kawakami, S.; Yamashita, F.; Hashida, M. Development of an antigen-presenting cell-targeted DNA vaccine against melanoma by mannosylated liposomes. *Biomaterials* 2007, *28*, 3255–3262.

(20) Sakurai, F.; Inoue, R.; Nishino, Y.; Okuda, A.; Matsumoto, O.; Taga, T.; Yamashita, F.; Takakura, Y.; Hashida, M. Effect of DNA/liposome mixing ratio on the physicochemical characteristics, cellular uptake and intracellular trafficking of plasmid DNA/cationic liposome complexes and subsequent gene expression. *J. Controlled Release* 2000, *66*, 255–269.

(21) Kalat, M.; Küpcü, Z.; Schüller, S.; Zalusky, D.; Zehetner, M.; Paster, W.; Schweighoffer, T. In vivo plasmid electroporation induces tumor antigen-specific CD8$^+$ T-cell responses and delays tumor growth in a syngeneic mouse melanoma model. *Cancer Res.* 2002, *62*, 5489–5494.

(22) Yamaoka, A.; Guan, X.; Takemoto, S.; Nishikawa, M.; Takakura, Y. Development of a novel Hsp70-based DNA vaccine as a multifunctional antigen delivery system. *J. Controlled Release* 2010, *142*, 411–415.

(23) Silver, P. B.; Agarwal, R. K.; Su, S. B.; Suffia, I.; Grajewski, R. S.; Luger, D.; Chan, C. C.; Mahdi, R. M.; Nickerson, J. M.; Caspi, R. R. Hydrodynamic vaccination with DNA encoding an immunologically privileged retinal antigen protects from autoimmunity through induction of regulatory T cells. *J. Immunol.* 2007, *179*, 5146–5158.

(24) Neal, Z. C.; Bates, M. K.; Albertini, M. R.; Herweijer, H. Hydrodynamic limb vein delivery of a xenogeneic DNA cancer vaccine effectively induces antitumor immunity. *Mol. Ther.* 2007, *15*, 422–430.

(25) Suzuki, R.; Oda, Y.; Utoguchi, N.; Namai, E.; Taira, Y.; Okada, N.; Kadowaki, N.; Kodama, T.; Tachibana, K.; Maruyama, K. A novel strategy utilizing ultrasound for antigen delivery in dendritic cell-based cancer immunotherapy. *J. Controlled Release* 2009, *133*, 198–205.

(26) Somiari, S.; Glasspool-Malone, J.; Drabick, J. J.; Gilbert, R. A.; Heller, R.; Jaroszeski, M. J.; Malone, R. W. Theory and in vivo application of electroporative gene delivery. *Mol. Ther.* 2000, *2*, 178–187.

(27) Kobayashi, N.; Kuramoto, T.; Yamaoka, K.; Hashida, M.; Takakura, Y. Hepatic uptake and gene expression mechanisms following intravenous administration of plasmid DNA by conventional and hydrodynamics-based procedures. *J. Pharmacol. Exp. Ther.* 2001, *297*, 853–860.

(28) Budker, V. G.; Subbotin, V. M.; Budker, T.; Sebestyén, M. G.; Zhang, G.; Wolff, J. A. Mechanism of plasmid delivery by hydrodynamic

tail vein injection. II. Morphological studies. *J. Gene Med.* **2006**, *8*, 874–888.

(29) Negishi, Y.; Endo, Y.; Fukuyama, T.; Suzuki, R.; Takizawa, T.; Omata, D.; Maruyama, K.; Aramaki, Y. Delivery of siRNA into the cytoplasm by liposomal bubbles and ultrasound. *J. Controlled Release* **2008**, *132*, 124–130.

(30) Hernot, S.; Klibanov, A. L. Microbubbles in ultrasound-triggered drug and gene delivery. *Adv. Drug Delivery Rev.* **2008**, *60*, 1153–1166.

(31) Tlaxca, J. L.; Anderson, C. R.; Klibanov, A. L.; Lowrey, B.; Hossack, J. A.; Alexander, J. S.; Lawrence, M. B.; Rychak, J. J. Analysis of in vitro Transfection by Sonoporation Using Cationic and Neutral Microbubbles. *Ultrasound Med. Biol.* **2010**, *36*, 1907–1918.

(32) Un, K.; Kawakami, S.; Suzuki, R.; Maruyama, K.; Yamashita, F.; Hashida, M. Enhanced transfection efficiency into macrophages and dendritic cells by a combination method using mannosylated lipoplexes and bubble liposomes with ultrasound exposure. *Hum. Gene Ther.* **2010**, *21*, 65–74.

(33) Un, K.; Kawakami, S.; Suzuki, R.; Maruyama, K.; Yamashita, F.; Hashida, M. Development of an ultrasound-responsive and mannose-modified gene carrier for DNA vaccine therapy. *Biomaterials* **2010**, *31*, 7813–7826.

(34) Bellone, M.; Cantarella, D.; Castiglioni, P.; Crosti, M. C.; Ronchetti, A.; Moro, M.; Garancini, M. P.; Casorati, G.; Dellabona, P. Relevance of the tumor antigen in the validation of three vaccination strategies for melanoma. *J. Immunol.* **2000**, *165*, 2651–2656.

(35) Xiang, R.; Lode, H. N.; Chao, T. H.; Ruehlmann, J. M.; Dolman, C. S.; Rodriguez, F.; Whitton, J. L.; Overwijk, W. W.; Restifo, N. P.; Reisfeld, R. A. An autologous oral DNA vaccine protects against murine melanoma. *Proc. Natl. Acad. Sci. U.S.A.* **2000**, *97*, 5492–5497.

(36) Hyoudou, K.; Nishikawa, M.; Umeyama, Y.; Kobayashi, Y.; Yamashita, F.; Hashida, M. Inhibition of metastatic tumor growth in mouse lung by repeated administration of polyethylene glycol-conjugated catalase: quantitative analysis with firefly luciferase-expressing melanoma cells. *Clin. Cancer Res.* **2004**, *10*, 7685–7691.

(37) Hyoudou, K.; Nishikawa, M.; Kobayashi, Y.; Kuramoto, Y.; Yamashita, F.; Hashida, M. Inhibition of adhesion and proliferation of peritoneally disseminated tumor cells by pegylated catalase. *Clin. Exp. Metastasis* **2006**, *23*, 269–278.

(38) Steinman, R. M.; Banchereau, J. Taking dendritic cells into medicine. *Nature* **2007**, *449*, 419–426.

(39) Mortimer, I.; Tam, P.; MacLachlan, I.; Graham, R. W.; Saravolac, E. G.; Joshi, P. B. Cationic lipid-mediated transfection of cells in culture requires mitotic activity. *Gene Ther.* **1999**, *6*, 403–411.

(40) Zou, S.; Scarfo, K.; Nantz, M. H.; Hecker, J. G. Lipid-mediated delivery of RNA is more efficient than delivery of DNA in non-dividing cells. *Int. J. Pharm.* **2010**, *389*, 232–243.

(41) Filion, M. C.; Phillips, N. C. Toxicity and immunomodulatory activity of liposomal vectors formulated with cationic lipids toward immune effector cells. *Biochim. Biophys. Acta* **1997**, *1329*, 345–356.

(42) Bolondi, L.; Correas, J. M.; Lencioni, R.; Weskott, H. P.; Piscaglia, F. New perspectives for the use of contrast-enhanced liver ultrasound in clinical practice. *Dig. Liver Dis.* **2007**, *39*, 187–195.

(43) Piscaglia, F.; Lencioni, R.; Sagrini, E.; Pina, C. D.; Cioni, D.; Vidili, G.; Bolondi, L. Characterization of focal liver lesions with contrast-enhanced ultrasound. *Ultrasound Med. Biol.* **2010**, *36*, 531–550.

(44) Tsivgoulis, G.; Culp, W. C.; Alexandrov, A. V. Ultrasound enhanced thrombolysis in acute arterial ischemia. *Ultrasonics* **2008**, *48*, 303–311.

(45) Siegel, R. J.; Luo, H. Ultrasound thrombolysis. *Ultrasonics* **2008**, *48*, 312–320.

(46) Kurts, C. CD11c: not merely a murine DC marker, but also a useful vaccination target. *Eur. J. Immunol.* **2008**, *38*, 2072–2075.

(47) Dredge, K.; Marriott, J. B.; Todryk, S. M.; Dalgleish, A. G. Adjuvants and the promotion of Th1-type cytokines in tumour immunotherapy. *Cancer Immunol. Immunother.* **2002**, *51*, 521–531.

(48) Hurpin, C.; Rotarioa, C.; Bisceglia, H.; Chevalier, M.; Tartaglia, J.; Erdile, L. The mode of presentation and route of administration are critical for the induction of immune responses to p53 and antitumor immunity. *Vaccine* **1998**, *16*, 208–215.

(49) Guan, X.; Nishikawa, M.; Takemoto, S.; Ohno, Y.; Yata, T.; Takakura, Y. Injection site-dependent induction of immune response by DNA vaccine: comparison of skin and spleen as a target for vaccination. *J. Gene Med.* **2010**, *12*, 301–309.

RESEARCH PAPER

Delivery of an Angiogenic Gene into Ischemic Muscle by Novel Bubble Liposomes Followed by Ultrasound Exposure

Yoichi Negishi • Keiko Matsuo • Yoko Endo-Takahashi • Kentaro Suzuki • Yuuki Matsuki • Norio Takagi • Ryo Suzuki • Kazuo Maruyama • Yukihiko Aramaki

ABSTRACT

Purpose To develop a safe and efficient gene delivery system into skeletal muscle using the combination of Bubble liposomes (BL) and ultrasound (US) exposure, and to assess the feasibility and the effectiveness of BL for angiogenic gene delivery in clinical use.

Methods A solution of luciferase-expressing plasmid DNA (pDNA) and BL was injected into the tibialis (TA) muscle, and US was immediately applied to the injection site. The transfection efficiency was estimated by a luciferase assay. The ischemic hindlimb was also treated with BL and US-mediated intramuscular gene transfer of bFGF-expressing plasmid DNA. Capillary vessels were assessed using immunostaining. The blood flow was determined using a laser Doppler blood flow meter.

Results Highly efficient gene transfer could be achieved in the muscle transfected with BLs, and US mediated the gene transfer. Capillary vessels were enhanced in the treatment groups with this gene transfer method. The blood flow in the treated groups with this gene transfer method quickly recovered compared to other treatment groups (non-treated, bFGF alone, or bFGF+US).

Conclusion The gene transfer system into skeletal muscle using the combination of BL and US exposure could be an effective means for angiogenic gene therapy in limb ischemia.

KEY WORDS angiogenesis · bubble liposomes · gene delivery · ultrasound

INTRODUCTION

Skeletal muscle is a candidate target tissue for the gene therapy of both muscle (*e.g.*, Duschenne Muscular dystrophy) and non-muscle disorders (*e.g.*, cancer, ischemia, or arthritis). Its usefulness is due mainly to its stability and longevity after a gene transfer, which make it a good target tissue for gene therapy via the production of therapeutic proteins such as cytoskeletal proteins, trophic factors, or hormones. To achieve successful gene therapy in a clinical setting, it is critical that gene delivery systems be safe, easy to apply, and provide therapeutic transgene expression. Several previous studies using viral vectors reported the successful transfer of therapeutic genes into the target cells, but because of the considerable immunogenicity related to the use of viruses, non-viral gene transfer still needs to be developed (1). Recently, among physical non-viral gene transfer methods, it has been shown that therapeutic ultrasound enables genes to permeate cell membranes. The mechanism of gene transfer is believed to be involved in an acoustic cavitation (2–6). However, to achieve efficient gene transfer, a high

Yoichi Negishi and Keiko Matsuo have contributed equally to this work.

Y. Negishi (✉) • K. Matsuo • Y. Endo-Takahashi • K. Suzuki • Y. Matsuki • Y. Aramaki
Department of Drug and Gene Delivery Systems
School of Pharmacy, Tokyo University of Pharmacy and Life Sciences
1432-1 Horinouchi, Hachioji
Tokyo 192-0392, Japan
e-mail: negishi@toyaku.ac.jp

N. Takagi
Department of Molecular and Cellular Pharmacology
School of Pharmacy, Tokyo University of Pharmacy and Life Sciences
1432-1 Horinouchi, Hachioji
Tokyo 192-0392, Japan

R. Suzuki • K. Maruyama
Department of Pharmaceutics, Teikyo University
1091-1 Suwarashi, Midori-ku
Sagamihara, Kanagawa 252-5195, Japan

intensity of US is required, which leads to tissue damage (7,8). In contrast, low-intensity US in combination with microbubbles has recently acquired much attention as a safe method of gene delivery (9–13). However, micro-bubbles have problems with size, stability, and targeting function. Liposomes have been known as drug, antigen, and gene delivery carriers (14–18). To solve the above-mentioned issues of microbubbles, we previously developed the polyethyleneglycol (PEG)-modified liposomes entrapping echo-contrast, "bubble liposomes" (BL), which can function as a novel gene delivery tool by applying them with US exposure (19–24).

In the present study, we developed a safe and efficient gene delivery system into skeletal muscle using the combination of BL and US exposure. We assessed the feasibility and the effectiveness of BL for gene therapy by trying to deliver a bFGF-expressing plasmid into skeletal muscle in a hindlimb ischemia model through the combination of BL and US exposure.

MATERIALS AND METHODS

Materials

Preparation of Bubble Liposomes

Bubble liposomes were prepared by the previously described methods (19,22). Briefly, PEG liposomes composed of 1, 2-dipalmitoyl-*sn*-glycero-3-phosphocholine (DPPC) (NOF Corporation, Tokyo, Japan) and 1,2-distearoyl-*sn*-glycero-3-phosphatidyl-ethanolamine-polyethyleneglycol (DSPE-PEG$_{2000}$-OMe) (NOF corporation, Tokyo, Japan) in a molar ratio of 94:6 were prepared by a reverse phase evaporation method. In brief, all reagents were dissolved in 1:1 (v/v) chloroform/diisopropyl ether. Phosphate-buffered saline was added to the lipid solution, and the mixture was sonicated and then evaporated at 47°C. The organic solvent was completely removed, and the size of the liposomes was adjusted to less than 200 nm using extruding equipment and a sizing filter (pore size: 200 nm) (Nuclepore Track-Etch Membrane, Whatman plc, UK). The lipid concentration was measured using a Phospholipid C test Wako (Wako Pure Chemical Industries, Ltd., Osaka, Japan). BL were prepared from liposomes and perfluoropropane gas (Takachio Chemical Ind. Co. Ltd., Tokyo, Japan). First, 2-mL sterilized vials containing 0.8 mL of liposome suspension (lipid concentration: 1 mg/mL) were filled with perfluoropropane gas, capped, and then pressurized with a further 3 mL of perfluoropropane gas. The vial was placed in a bath-type sonicator (42 kHz, 100 W) (BRANSONIC 2510j-DTH, Branson Ultrasonics Co., Danbury, CT, USA) for 5 min to form BL.

Plasmid DNA (pDNA)

The plasmid pcDNA3-Luc, derived from pGL3-basic (Promega, Madison, WI), is an expression vector encoding the firefly luciferase gene under the control of a cytomegalovirus promoter. The plasmid pEGFP-N3 (Clontech Laboratories, Inc., Mountain View, CA) is an expression vector encoding the enhanced green fluorescein protein under the control of a cytomegalovirus promoter. The plasmid pBLAST-hbFGF (InvivoGen Inc.) is an expression vector encoding human bFGF under the control of an EF-1α promoter.

In Vivo Gene Delivery into the Skeletal Muscle of Mice with BL and US

ICR mice (5 weeks old, male) were anesthetized with pentobarbital throughout each procedure. A 40 μl suspension of pDNA (10 μg) and BL (30 μg) was injected into the tibialis (TA) muscle of the ICR mice, and US exposure (frequency: 1 MHz; duty: 50%; intensity: 2 W/cm^2; time: 60 s) was immediately applied at the injection site. A Sonitron 2000 (NEPA GENE, CO, LTD) was used as an ultrasound generator. Several days after the injection, the mice were euthanized and sacrificed, and the tibialis muscle in the US-exposed area was collected and homogenized. The cell lysate and tissue homogenates were prepared with a lysis buffer (0.1 M Tris-HCl (pH 7.8), 0.1% Triton X-100, and 2 mM EDTA). Luciferase activity was measured using a luciferase assay system (Promega, Madison, WI) and a luminometer (LB96V, Belthold Japan Co. Ltd., Tokyo, Japan). The activity is indicated as relative light units (RLU) per mg of protein. For analyzing EGFP expression, the treated muscle was fixed with paraformaldehyde and dehydrated in a sucrose solution. The specimens were embedded in an OCT compound and immediately frozen at −80°C. Serial sections 8 μm thick were cut by cryostat and observed with a fluorescence microscope (Axiovert 200 M, Carl Zeiss).

In Vivo Luciferase Imaging

The mice were anaesthetized and *i.p.* injected with D-luciferin (150 mg/kg) (Xenogen, Corporation, CA). After 10 min, luciferase expression was observed with an *in vivo* luciferase imaging system (IVIS) (Xenogen Corporation).

Tissue-Damage Testing Using Evans-Blue Dye (EBD)

Tissue-damage testing using EBD was performed as previously reported (25). Briefly, EBD was dissolved in PBS (10 mg/ml) and sterilized by using 0.2 μm membrane filters. Mice treated with pDNA, BL, and US exposure were administered with the dissolved EBD (0.5 mg dye per